UNIVERSITY OF BIRMINGHAM
University of Birmingham Research at Birmingham

Genotype-phenotype correlation in Junctional Epidermolysis Bullosa

Wen, David; Hunjan, Manrup; Bardhan, Ajoy; Harper, Natasha; Ogboli, Malobi; Ozoemena, Linda; Fine, Jo-David; Chapple, Iain; Balacco, Dario; Heagerty, Adrian

DOI:
10.1016/j.jid.2023.11.021

License:
Creative Commons: Attribution (CC BY)

Document Version
Version created as part of publication process; publisher's layout; not normally made publicly available

Citation for published version (Harvard):
Wen, D, Hunjan, M, Bardhan, A, Harper, N, Ogboli, M, Ozoemena, L, Fine, J-D, Chapple, I, Balacco, D & Heagerty, A 2023, 'Genotype-phenotype correlation in Junctional Epidermolysis Bullosa: signposts to severity', *Journal of Investigative Dermatology*. https://doi.org/10.1016/j.jid.2023.11.021

Link to publication on Research at Birmingham portal

General rights
Unless a licence is specified above, all rights (including copyright and moral rights) in this document are retained by the authors and/or the copyright holders. The express permission of the copyright holder must be obtained for any use of this material other than for purposes permitted by law.

•Users may freely distribute the URL that is used to identify this publication.
•Users may download and/or print one copy of the publication from the University of Birmingham research portal for the purpose of private study or non-commercial research.
•User may use extracts from the document in line with the concept of 'fair dealing' under the Copyright, Designs and Patents Act 1988 (?)
•Users may not further distribute the material nor use it for the purposes of commercial gain.

Where a licence is displayed above, please note the terms and conditions of the licence govern your use of this document.

When citing, please reference the published version.

Take down policy
While the University of Birmingham exercises care and attention in making items available there are rare occasions when an item has been uploaded in error or has been deemed to be commercially or otherwise sensitive.

If you believe that this is the case for this document, please contact UBIRA@lists.bham.ac.uk providing details and we will remove access to the work immediately and investigate.

Download date: 10. Jan. 2024

Journal Pre-proof

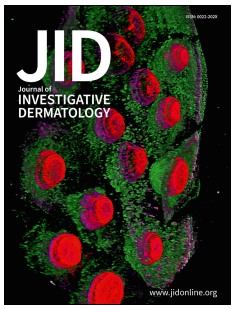

Genotype-phenotype correlation in Junctional Epidermolysis Bullosa: signposts to severity

Dr David Wen, Dr Manrup Hunjan, Dr Ajoy Bardhan, Dr Natasha Harper, Dr Malobi Ogboli, Dr Linda Ozoemena, Dr Lu Liu, Jo-David Fine, Professor, Iain Chapple, Professor, Dr Dario L. Balacco, Adrian Heagerty, Professor

PII: S0022-202X(23)03205-0

DOI: https://doi.org/10.1016/j.jid.2023.11.021

Reference: JID 4108

To appear in: *The Journal of Investigative Dermatology*

Received Date: 18 May 2023

Revised Date: 10 October 2023

Accepted Date: 9 November 2023

Please cite this article as: Wen D, Hunjan M, Bardhan A, Harper N, Ogboli M, Ozoemena L, Liu L, Fine J-D, Chapple I, Balacco DL, Heagerty A, Genotype-phenotype correlation in Junctional Epidermolysis Bullosa: signposts to severity, *The Journal of Investigative Dermatology* (2024), doi: https://doi.org/10.1016/j.jid.2023.11.021.

This is a PDF file of an article that has undergone enhancements after acceptance, such as the addition of a cover page and metadata, and formatting for readability, but it is not yet the definitive version of record. This version will undergo additional copyediting, typesetting and review before it is published in its final form, but we are providing this version to give early visibility of the article. Please note that, during the production process, errors may be discovered which could affect the content, and all legal disclaimers that apply to the journal pertain.

© 2023 The Authors. Published by Elsevier, Inc. on behalf of the Society for Investigative Dermatology.

Genotype-phenotype correlation in Junctional Epidermolysis Bullosa: signposts to severity

Short title: Genotype-phenotype correlation in Junctional EB

Keywords: LAMB3, laminin 332, COL17A1, bioinformatics, genomics

Word count: 3,674

Table count: 3

Figure count: 3

Authors and institutions

Dr David Wen[1,2,3,4], Dr Manrup Hunjan[1,2,5], Dr Ajoy Bardhan[1,2], Dr Natasha Harper[2], Dr Malobi Ogboli[6], Dr Linda Ozoemena[7], Dr Lu Liu[7], Professor Jo-David Fine[8], Professor Iain Chapple[1,9,10], Dr Dario L. Balacco[1] *, Professor Adrian Heagerty[2,11] *

* = Joint last authors

[1]Institute of Clinical Sciences, University of Birmingham, Birmingham, United Kingdom.

[2]Adult Epidermolysis Bullosa Unit, Department of Dermatology, University Hospitals Birmingham NHS Foundation Trust, Birmingham, United Kingdom.

[3]Oxford University Clinical Academic Graduate School, University of Oxford, Oxford, United Kingdom.

[4]Oxford University Hospitals NHS Foundation Trust, Oxford, United Kingdom.

[5]Department of Dermatology, Walsall Manor Hospital, Walsall, United Kingdom.

[6]Paediatric Epidermolysis Bullosa Unit, Department of Paediatric Dermatology, Birmingham Children's Hospital NHS Foundation Trust, Birmingham, United Kingdom.

[7]National Diagnostic EB Laboratory, Synovis, St Thomas' Hospital, London, United Kingdom.

[8]Department of Dermatology, Vanderbilt University Medical Centre, Nashville, Tennessee, United States of America.

[9]Birmingham Dental Hospital, Birmingham Community Health NHS Foundation Trust, Birmingham, United Kingdom.

[10]Birmingham NIHR BRC Inflammation Research, Birmingham, United Kingdom.

[11]Institute of Inflammation and Ageing, University of Birmingham, Birmingham, United Kingdom.

Corresponding author: Dr David Wen, david.wen@nhs.net
ORCID: 0000-0001-9112-8517
Department of Dermatology, Churchill Hospital Old Road, Oxford, United Kingdom, OX3 7LE

ORCIDs:

David Wen ORCID: 0000-0001-9112-8517
Manrup Hunjan ORCID: 0000-0003-4620-6082
Ajoy Bardhan ORCID: 0000-0001-8281-6123
Natasha Harper ORCID: 0000-0002-8093-2160
Malobi Ogboli ORCID: 0000-0002-8861-6998

Journal Pre-proof

Linda Ozoemena ORCID: 0009-0006-8554-6652
Lu Liu ORCID: 0000-0002-2547-9850
Jo-David Fine ORCID: 0009-0005-9415-8646
Iain Chapple ORCID: 0000-0003-2697-7082
Dario Leonardo Balacco ORCID: 0000-0002-7648-1213
Adrian Heagerty ORCID: 0000-0003-4351-7467

Twitter handles:
Dr Dario L. Balacco : @dariobalacco
Dr Ajoy Bardhan: @ajoyb_

Abbreviations used:
Junctional epidermolysis bullosa (JEB)
Loss-of-function (LoF)
Nonsense-mediated decay (NMD)
Premature termination codon (PTC)

This work was completed in Birmingham, West Midlands, United Kingdom and London, United Kingdom.

Journal Pre-proof

Journal Pre-proof

Abstract

Junctional epidermolysis bullosa (JEB) is a rare autosomal recessive genodermatosis with a broad spectrum of phenotypes. Current genotype-phenotype paradigms are insufficient to accurately predict JEB subtype and characteristics from genotype, particularly for splice site mutations, which account for over a fifth of disease-causing mutations in JEB. This study evaluated genetic and clinical findings from a JEB cohort, investigating genotype-phenotype correlations through bioinformatic analyses and comparison with previously reported mutations.

Eighteen unique mutations in *LAMB3*, *LAMA3*, *LAMC2* or *COL17A1* were identified from seventeen individuals. Seven had severe JEB, nine intermediate JEB and one laryngo-onycho-cutaneous syndrome. Seven mutations were previously unreported. Deep phenotyping was completed for all intermediate JEB cases and demonstrated substantial variation between individuals. Splice site mutations underwent analysis with SpliceAI, a state-of-the-art artificial intelligence tool, in order to predict resultant transcripts. Predicted functional effects included exon skipping and cryptic splice site activation, which provided potential explanations for disease severity and in most cases correlated with lamimin-332 immunofluorescence. RT-PCR was performed for one case to investigate resultant transcripts produced from the splice site mutation.

This study expands the JEB genomic and phenotypic landscape. AI tools show potential for predicting functional effects of splice site mutations and may identify candidates for confirmatory laboratory investigation. Investigation of RNA transcripts will help to further elucidate genotype-phenotype correlations for novel mutations.

Introduction

Junctional epidermolysis bullosa (JEB) is a rare autosomal recessive genodermatosis characterised by mucocutaneous cleavage within the lamina lucida of the basement membrane zone (Bardhan et al., 2020). Currently, mutations in seven genes have been identified to result in JEB. Laminin-332 is the most commonly mutated protein in JEB, and is a heterotrimer composed of α3, β3 and γ2 chains, which are encoded by *LAMA3*, *LAMB3* and *LAMC2* respectively (Has et al., 2020).

Two main subtypes of JEB exist with varying clinical courses. Children born with severe JEB often do not survive past the first few years of life, due to the severity of mucocutaneous blistering and extracutaneous manifestations (Varki et al., 2006). Individuals with intermediate JEB follow a different clinical course and usually survive into adulthood, with heterogenous clinical manifestations of varying severity and tissue types affected (Has et al., 2020).

Classical genotype-phenotype correlation paradigms predict that in most cases, severe JEB arises from biallelic loss-of-function (LoF) premature termination codon (PTC) mutations in *LAMA3*, *LAMB3* or *LAMC2*, which result in nonsense-mediated decay (NMD) of mRNA transcripts, or production of truncated non-functional polypeptides (Nakano et al., 2002). In contrast, most intermediate JEB cases with mutations in the laminin-332 genes are caused by compound heterozygosity for a PTC mutation and a non-LoF mutation, or biallelic non-LoF mutations (Has and Bruckner-Tuderman, 2014, Nakano et al., 2000). Indeed, it has been demonstrated that only a small amount of functional or partially functional laminin polypeptide (5–10% of residual protein) can considerably ameliorate disease severity (Has et al., 2020). In

addition, biallelic mutations in *COL17A1* generally also result in intermediate JEB (Has et al., 2020).

Splice site mutations account for over one fifth of disease-causing mutations in JEB (HGMD Professional 2021.1, Stenson et al., 2020) affecting pre-mRNA splicing through activation of cryptic splice sites and/or exon skipping. Predicting the precise location of activated cryptic splice sites is vital, as these can produce out-of-frame transcripts and PTCs, which undergo NMD or translation into truncated proteins with limited or no functionality, often correlated with severe JEB.

Importantly, these paradigms are not generalisable to all JEB cases. A minority of JEB patients have been reported to have biallelic LoF PTC mutations in the laminin-332 genes with a corresponding intermediate JEB phenotype rather than the expected severe JEB phenotype. Mechanisms demonstrated include in-frame exon skipping (McGrath et al., 1999, Nakano et al., 2002), PTC readthrough (Pacho et al., 2011), and rescue of pre-existing mRNA isoforms due to reframing of naturally occurring out-of-frame transcripts, exemplified by the c.1587delAG mutation in *LAMB3* (Gache et al., 2001, Posteraro et al., 2004).

Current genotype-phenotype paradigms are insufficient to accurately predict JEB subtype, characteristics and prognosis from genotype, with implications for patients, families and clinical services. This study aimed to evaluate genetic and clinical findings from a JEB cohort; genotype-phenotype correlations were investigated using an approach utilising bioinformatic tools that previously have not been applied to this condition, along with comparison to reported cases in the literature.

Results

Cohort characteristics and genotypes

The study cohort consisted of 13 homozygotes and 4 compound heterozygotes with 21 mutations in total (Table 1). Of the 17 individuals, 7 had severe JEB (all deceased), 1 had laryngo-onycho-cutaneous (LOC) syndrome (deceased) and 9 had intermediate JEB (all living). Most mutations were in *LAMB3* (12 of 21, 57%), and were nonsense or out-of-frame indel mutations (14 of 21, 67%). 5 of 21 mutations (24%) were splice site mutations (Figure 1).

A few individuals had the same genotypes. Cases 12 and 13 had the same four nucleotide deletion in *LAMC2*, Cases 14 and 15 had the same single nucleotide insertion in *COL17A1*, and Cases 16 and 17 had the same large deletion in *COL17A1*. Therefore, of the 21 mutations identified in the cohort, 18 were unique. Seven mutations, that to our knowledge were previously unreported, were identified (Supplementary Table S1). *LAMB3* (Figure 2), *LAMA3*, *LAMC2*, and *COL17A1* mutations (Supplementary Figure S1a–c) were mapped onto gene, transcript and protein plots. Predicted InterPro protein domains of protein schematics and their significance scores are shown in Supplementary Table S2.

Immunofluorescence mapping

Immunofluorescence mapping (IFM) was completed for 10 of 17 participants (Supplementary Table S3). Staining with GB3 antibody (Heagerty et al., 1986) was completely absent in severe JEB cases, and was diminished in intensity and interrupted in distribution for intermediate JEB cases. The GB3 antibody recognises an epitope located within the γ2 chain of laminin-332, although a stable laminin 332 heterotrimer is a prerequisite for staining (Matsui et al., 1995). Mutations affecting the α3 and β3 chains destabilise the laminin-332 heterotrimer, obscuring

the GB3 epitope (Matsui et al., 1995), and so additional immunofluorescence staining for other chains is not routinely performed.

Intermediate JEB deep phenotyping

Deep phenotyping of nine intermediate JEB individuals revealed substantial variation (Table 2). Skin area affected varied from 0% to 51–60%. All individuals' nails were affected with scores ranging from 2.5 to 5 (all nails lost). Ocular involvement, chronic wounds, tooth damage or loss, oral ulcers, scarring alopecia, atrophic scarring, anaemia and being underweight were also common (>50% of cases). Hypoalbuminaemia, laryngeal involvement and presence of granulation tissue were less common (<50% of cases). Case 16 was the only individual who experienced a life-threatening illness (sepsis). Individuals with severe JEB and LOC syndrome were deceased at the time of the study and did not undergo deep phenotyping.

Analysis of *LAMB3* splice site variants using SpliceAI

Five unique splice site mutations were identified in the cohort which were all found in *LAMB3*. To investigate whether prediction scores for gain or loss sites changed with -D (i.e., the maximum distance between the variant and a gain or loss site), repeat analyses were performed with different -D parameters, outlined in Supplementary Table S4. No further delta score changes occurred beyond -D of 150nt. This is likely due to the size of -D (150nt) corresponding to the length of exon 18 (145nt), which was the longest exon to be affected by a splice site mutation (Case 7, *LAMB3* c.2701+1G>A).

SpliceAI delta scores for each splice site mutation are summarised in schematic diagrams (Supplementary Figure S2a-e). Potential resultant transcripts predicted are summarised in Table

3. For Case 7 (*LAMB3* c.2701+1G>A/c.2701+1G>A), SpliceAI predicted out-of-frame transcripts containing PTCs following exon skipping or cryptic splice site activation. Regarding Case 8 (*LAMB3* c.565-2A>G/p.R972X), an out-of-frame transcript was predicted secondary to exon 7 skipping, and an in-frame transcript was predicted following cryptic splice site activation within intron 6. However, when translated, this transcript contained a TGA termination codon at position c.565-60 (Supplementary Table S5, Supplementary Figure S3). Therefore, for both of these individuals, the splice site mutations were likely to produce no functional protein, which correlated with lack of immunoreactivity for GB3 on IFM (Supplementary Figure S4a-b) and these individuals' severe JEB phenotypes.

An in-frame transcript with 27 additional nucleotides was predicted for Case 9 (*LAMB3* c.943+2T>C/p.R569X) secondary to cryptic splice site activation within intron 9. This likely produced some partially functional protein and mitigated JEB severity, explaining reduced but present immunoreactivity for GB3 on IFM (Supplementary Figure S4c), and her mild intermediate JEB phenotype with minimal skin involvement.

In Case 10 (*LAMB3* c.629-12T>A/p.W1040X), cryptic splice site activation within intron 7 was strongly predicted, which would lead to inclusion of 10nt from intron 7 between exons 7 and 8, resulting in a frameshift. Nevertheless, this individual had an intermediate JEB phenotype. Notably, Hou et al. reported this mutation and confirmed that it activated a cryptic splice site in intron 7, adding 10 nucleotides, (Hou et al., 2021) consistent with SpliceAI's prediction. However, this was a leaky splice site, resulting in alternate splicing producing both wild type and mutant transcripts in a 1:3–1:7 ratio, which may explain the intermediate JEB phenotype observed in Case 10.

Journal Pre-proof

For Case 11 (*LAMB3* c.298+5G>C), cryptic splice site activation (with inclusion of 64nt from intron 4) or exon 4 skipping was predicted to produce out-of-frame transcripts and severe JEB phenotype. Nevertheless, this individual exhibited an intermediate JEB phenotype, along with slight immunoreactivity for GB3 on IFM (Figure S4d-e), and so further investigation was warranted.

RNA transcript analysis of Case 11

RT-PCR of mRNA extracted from white blood cells confirmed the presence of *LAMB3* transcript A (Supplementary Figure S5), which contained an additional 64nt of intron 4 between exons 4 and 5. RT-PCR of skin biopsy samples detected both transcript A and an additional minor transcript, transcript B, which contained an additional 60nt of intron 4 between exons 4 and 5 (Supplementary Figure S6a-b). Transcript B would generate an in-frame transcript with an additional 20 amino acids at position p.100.

To generate transcript B, a donor splice site at c.298+60 would be required (splice site B, Supplementary Figure S7). As SpliceAI only gives one donor gain score for the strongest gain site within -D (in this case c.298+64 with -D of 150nt), targeted SpliceAI analysis with -D of 58nt was performed to determine if the c.298+5G>C mutation would increase the likelihood of c.298+60 being used as a splice site. All nucleotides from c.298+1-c.298+63 within intron 4 would be considered, but not c.298+64 (Supplementary Figure S8). A minimal donor gain of 0.01 was predicted at c.295+32 (Supplementary Table S6), suggesting that c.298+60 (splice site B) was not a strong splice site.

The wild type sequence flanking splice site B is TG|GA (Supplementary Figure S7). The GA dinucleotide appears to be poorly suited to being a donor splice site, as it does not follow the

GT-AG rule, where the vast majority of donor splice sites are delineated with a consensus GT dinucleotide (Breathnach et al., 1978). Therefore, it was hypothesised that a second mutation (A>T) at c.295+62 in a small population of cells could create a more suitable splice site, TG|GT, and increase the likelihood of generating a cryptic splice site to produce transcript B (Supplementary Figure S9). SpliceAI analysis was re-run with c.298+62A>T. However, as SpliceAI can only analyse one mutation at a time, this mutation could not be analysed together with c.298+5G>C. Nevertheless, analysis of c.298+62A>T in isolation predicted activation of a cryptic splice site at c.298+60, with a strong donor gain score of +0.94 (Supplementary Table S7).

To confirm whether the hypothesised second mutation was present (c.298+62A>T), intron 4 was sequenced. However, no second mutation was found at position c.298+62 on Sanger sequencing of blood and skin samples of blistered and non-blistered skin, raising the possibility that non-canonical splicing may produce transcript B.

Effects of exonic mutations on splicing

Two individuals with PTC mutations in *LAMB3* (Cases 5 and 6) are notable as they resulted in intermediate JEB. In addition to altering the primary sequence of a polypeptide, exonic mutations can also affect splicing. Natural in-frame skipping of the mutation bearing exon has been shown to be a mechanism that can eliminate PTCs, ameliorating JEB severity (McGrath et al., 1999). Mutations of Cases 5 and 6 were analysed using SpliceAI to determine if the mutations affected nearby splicing (Supplementary Table S8). Splicing alteration was virtually negligible for Case 6, with gain and loss scores of 0.01 only. Regarding Case 5, there was modest prediction (0.1) for an acceptor cryptic splice site at position c.1759 (161nt from the original intron 13 / exon 14 junction), with minimal disruption to the original acceptor splice

site (acceptor loss 0.04). Even if a transcript was produced from this, it would be out-of-frame (Supplementary Figure S10), and *in silico* translation confirmed a PTC two codons downstream from the new acceptor site (p.A533DfsX3).

Journal Pre-proof

Discussion

Non splice site mutations

Excluding the five individuals with splice site mutations, 10 of 12 individuals followed classical genotype-phenotype correlation paradigms. Biallelic frameshift indels in *LAMA3* and *LAMC2* resulted in severe JEB (or LOC syndrome, Case 3). All four individuals with *COL17A1* mutations had intermediate JEB. Comparison of these mutations (Cases 1–4, Cases 12–17) with those reported in the literature is presented in the Supplementary Text. Interestingly, two individuals with PTC mutations in *LAMB3* (Cases 5 and 6) had milder-than-expected phenotypes. Considering the SpliceAI predictions (Supplementary Table S8), skipping of the mutation-bearing exon was unlikely to account for the relatively mild phenotype. Remarkably, regarding Case 5 (Q568X), individuals homozygous for the nearby mutation *LAMB3* c.1705C>T in the adjacent codon (p.R569X) have been reported to have a severe JEB phenotype with early lethality (Khan et al., 2021). In contrast, Case 5 remains alive at 21 years of age, and her skin biopsy had some immunoreactivity on staining with GB3. We therefore feel that she should be classified as intermediate JEB.

Regarding Case 6 (*LAMB3* c.1186_1196del, p.T396CfsX12), a nearby and similar 11nt deletion (*LAMB3* c.1188_1198del, p.G397VfsX11) resulted in severe JEB in a homozygote (Varki et al., 2006). In contrast, Case 6 has survived to 7 years of age which clinically is more in keeping with intermediate JEB. A similar region is deleted in both cases, with the PTCs located at the same site (Supplementary Figure S11). The net effect is that only one codon is altered, and this results in two different JEB subtypes. Whilst there is a GTG codon (cysteine) rather than a GAC codon (threonine) at p.396, the sequences' influence on non-coding, regulatory functions should also be considered for further investigation.

Readthrough of TGA PTCs has been reported as a mechanism where translation is preserved in JEB (Pacho et al., 2011); however the PTC and flanking sequences of Cases 5 and 6 do not match established consensus sequences for PTC readthrough suggested by Pacho et al ((A/T)(A/G)(T/C) TGA CTA). Whilst other consensus sequences may exist which could facilitate PTC readthrough, given the widespread skin involvement and severity in these two individuals, this is unlikely; the case reported by Pacho et al produced full length *LAMA3* transcript and laminin-332 on IFM, and was phenotypically very mild. Therefore, it is likely that these two variants result in intermediate JEB through other mechanisms. Prediction of NMD occurrence and analysis of the RNA transcripts of these individuals will undoubtedly shed light on this.

Analysis of RNA transcripts in genotype-phenotype correlation

This study highlights the importance of examining RNA transcripts in selected cases for accurate genotype-phenotype correlation. Artificial intelligence tools such as SpliceAI show potential for elucidating mechanisms for severity. They may facilitate selection of cases for further laboratory investigation and can guide which regions of genes or transcripts to sequence for confirmatory analyses.

In this study, SpliceAI was used to analyse five splice site mutations. RT-PCR was available for two mutations, one locally (c.298+5G>C, Case 11) and one (c.629-12T>A, Case 10) reported in the literature (Hou et al., 2021). Investigation and validation with larger numbers of cases will be required to explore the accuracy of these tools in predicting transcript outcomes from splice site mutations, and whether scores may correlate with the quantity of transcripts produced. Considering Case 11, SpliceAI appears to be limited in prediction of leaky splicing

effects. Despite an acceptor splice site donor loss score of -0.92, production of wild type transcript was able to alleviate severity and result in an intermediate JEB phenotype. Furthermore, SpliceAI is unable to directly predict regulatory elements of splicing, such as exonic splicing enhancer motifs, disruption of which may result in alternative splicing, and potentially splicing out LoF mutations (McGrath et al., 1999).

In a recent study where computational tools were used to investigate the impact on splicing of 249 variants of unknown significance, SpliceAI outperformed seven other *in silico* splice mutation prediction tools (Rowlands et al., 2021). For this task, SpliceAI performance was greatest with a threshold of any delta score being greater than 0.145. Similar accuracy was found when SpliceAI was used to classify variants in the *NF1* gene with a delta score threshold of 0.22 (Ha et al., 2021).

Another limitation of SpliceAI is that only the single greatest delta score for each splice site category is given, potentially concealing other biologically significant predictions. Multiple transcripts and different expression levels may result from a splice site mutation, (Kiritsi et al., 2011, Nakano et al., 2002) with some transcripts being translated into functionally significant amounts of protein that could influence JEB severity (Hou et al., 2021). Therefore, techniques such as RNA-seq have utility in genotype-phenotype correlation investigation to identify different mRNA isoforms and their expression levels. Another benefit of RNA-seq is that up or down regulation of other genes encoding proteins which interact with laminin-332 can also be evaluated (Wang et al., 2009).

Finally, isoform expression in different tissues varies, and therefore splice site mutations may have different effects in different tissues, highlighted by different transcripts in blood and skin

of Case 11. Future models may address tissue-specific splice site mutation prediction (Jaganathan et al., 2019), potentially utilising data from the human cell atlas for model development (Regev et al., 2017).

JEB mutation database

This study also highlights the utility of a centralised database of JEB mutations and corresponding deep phenotypes which would be a vital resource for future predictions of severity. Due to the rarity of JEB, collation of cases is necessary for identification of disease patterns and genotype-phenotype relationships. Genotypes and corresponding phenotypes are often mentioned in individual articles, and as the data is disparate, it is arduous for clinicians and researchers to efficiently search and access data on genotypes and phenotypes in a single place. Therefore, mutation databases are required for comparison and analysis of data (Bardhan et al., 2020). In current databases, such as HGMD, nomenclature is outdated, limited phenotype information exists, and importantly data regarding both alleles (i.e. the full genotype) is not reported directly. Whilst a database for RDEB has been established (van den Akker et al., 2011), currently, no publicly available databases or registries exist specifically for JEB. Collation of sufficient cases in a database may allow deep genotype phenotype correlations to be drawn in the future.

Intermediate JEB Phenotyping

Different phenotypes within the intermediate JEB subtype were highlighted by variation in the presence and severity of characteristics. Atrophic scarring was observed in six individuals and may be considered for future JEB phenotyping systems. Limitations of phenotyping in this study include examination at one timepoint giving only a snapshot of disease activity and severity, and longitudinal phenotyping at standardised time points may allow more accurate

deep phenotype assessment and monitoring of disease course. Individuals with the same genotype (14 and 15, 16 and 17) had similar, but slightly different phenotypes, possibly due to changes with age, the presence of disease modifying factors, or both. The tool was limited in comparing scores between categories. Refinement could be achieved by using a structured methodology such as the Delphi method to achieve consensus opinion between experts (Engelman et al., 2018). Furthermore, formal testing and validation would be required before widespread use.

Conclusion

Accurate genotype-phenotype correlation has important clinical implications for JEB patients. Accurate predictions are challenging as a number of cases have a phenotype that is less severe than expected from their genetic defect, and this is also demonstrated in our cohort. *In silico* approaches show potential for analysis of functional effects of mutations and may identify candidates for confirmatory laboratory investigation. When further refined and validated, these computational tools may be suitable for routine clinical use. Concerning novel mutations, investigation of RNA transcripts will help to further elucidate genotype-phenotype correlations. Finally, the systematic approaches used in this study can be applied to available genetic data in the literature, and also other types of EB and other mendelian genetic diseases.

Journal Pre-proof

Materials and Methods

Setting and Subjects

The study was approved by the Health Research Authority (London Bridge Regional Ethics Committee) and was sponsored by University Hospitals Birmingham NHS Foundation Trust. Participants were recruited from two UK specialised EB units (Solihull Hospital and Birmingham Children's Hospital). Individuals diagnosed with JEB and with confirmed mutations in *LAMA3, LAMB3, LAMC2* or *COL17A1,* treated at either centre in the last 5 years were eligible for inclusion, including deceased patients. Written, informed consent was obtained from living patients or parents, in instances involving children. Patients unable to provide informed consent, or lacked a proxy were excluded from the study.

Laboratory investigations

Individuals underwent Sanger sequencing, WES, IFM and RT-PCR as part of their usual clinical care. Methods are previously described in Groves et al., 2010 and Takeichi et al., 2015. WES was used for one individual, as Sanger sequencing did not detect mutations in *LAMA3, LAMB3, LAMC2* or *COL17A1* initially. Data visualisation methods are outlined in the Supplementary Text.

SpliceAI analysis of splice site mutations

SpliceAI (Illumina, San Diego, California) is a 32-layer convolutional neural network which examines 10,000 nucleotides (nt) flanking a variant of interest to predict its effects on RNA splicing (Jaganathan et al., 2019). Changes in probabilities of positions being used as a splice

donor or acceptor in the presence of a mutation are given as four delta scores (donor loss, donor gain, acceptor loss and acceptor gain).

SpliceAI allows the user to set the maximum distance (-D) between the variant and a potential gain or loss site. To investigate whether prediction scores for gain or loss sites changed with -D, recurrent analyses were performed with different parameters of -D at 50, 100, 150, 200, 250, 350 and 4999 nucleotides.

Deep phenotyping of intermediate JEB patients

A modified version of the validated Birmingham Epidermolysis Bullosa Severity (BEBS) tool (Moss et al., 2009) was tailored to specifically deep phenotype individuals. Three previous EB expert consensus documents on EB classification and characteristics, along with relevant textbook chapters on JEB were reviewed for characteristic clinical features of intermediate and severe JEB (Barker et al., 2016, Fine et al., 2014, Fine et al., 2008, Has et al., 2020). Discussions were held between expert clinicians in EB (AH, ILC, JDF and AB) regarding pertinent phenotyping criteria. Additional items were added to the BEBS to allow better characterisation of JEB patients and their features. Categories irrelevant to JEB were removed from the tool. The phenotyping tool was piloted on three patients for ease of use, and the final version used in the study is shown in Figure 3. Scores for each category were not totalled into an overall score as whilst scores were comparable between individuals for the same category, scores across different categories did not lead to meaningful comparisons e.g. loss of all nails (nails score=5) does not equate to laryngeal obstruction (larynx score=5) or chronic wounds covering >40% body surface area (chronic wound score >5).

Acknowledgements: The authors would like to thank Alyson Guy from the National Diagnostic Epidermolysis Bullosa Laboratory for preparing the immunofluorescence mapping images.

Funding sources: This is independent research funded by the Dystrophic Epidermolysis Bullosa Research Association (DEBRA). The funder was not involved in the study design, data collection, data analysis or manuscript preparation.

Conflict of interests statement: all authors declare no competing interests.

Data availability statement: The authors confirm that the data supporting the findings of this study are available within the article and its supplementary materials.

The study was approved by the Health Research Authority (London Bridge Regional Ethics Committee) and was sponsored by University Hospitals Birmingham NHS Foundation Trust.

Author Contributions Statement:

Conceptualization: DW, AB, JDF, IC, DLB, AH;
Data Curation: DW, MH, AB, NH, MO, LO, LL;
Formal Analysis: DW, DLB;
Funding Acquisition: IC, AH;
Investigation: DW, MH, AB, NH, LO, LL, DLB;
Methodology: JDF, IC, DLB, AH;
Project Administration: DW, MO, IC, AH;
Resources: MH, AB, NH, MO, LO, LL, IC;
Software: DW, DLB;
Supervision: AB, IC, DLB, AH;
Visualization: DW, DLB;
Writing – Original Draft: DW, DLB;
Writing – Review & Editing: AB, NH, MO, LO, LL, JDF, IC, DLB, AH.

Journal Pre-proof

References

Bardhan A, Bruckner-Tuderman L, Chapple ILC, Fine JD, Harper N, Has C, et al. Epidermolysis bullosa. Nat Rev Dis Primers 2020;6(1):78.

Barker J, Bleiker TO, Chalmers R, Griffiths CEM, Creamer D. Rook's textbook of dermatology: John Wiley & Sons, 2016.

Breathnach R, Benoist C, O'Hare K, Gannon F, Chambon P. Ovalbumin gene: evidence for a leader sequence in mRNA and DNA sequences at the exon-intron boundaries. Proc Natl Acad Sci U S A 1978;75(10):4853-7.

Engelman D, Fuller LC, Steer AC, International Alliance for the Control of Scabies Delphi p. Consensus criteria for the diagnosis of scabies: A Delphi study of international experts. PLoS Negl Trop Dis 2018;12(5):e0006549.

Fine JD, Bruckner-Tuderman L, Eady RA, Bauer EA, Bauer JW, Has C, et al. Inherited epidermolysis bullosa: updated recommendations on diagnosis and classification. J Am Acad Dermatol 2014;70(6):1103-26.

Fine JD, Eady RA, Bauer EA, Bauer JW, Bruckner-Tuderman L, Heagerty A, et al. The classification of inherited epidermolysis bullosa (EB): Report of the Third International Consensus Meeting on Diagnosis and Classification of EB. J Am Acad Dermatol 2008;58(6):931-50.

Gache Y, Allegra M, Bodemer C, Pisani-Spadafora A, de Prost Y, Ortonne JP, et al. Genetic bases of severe junctional epidermolysis bullosa presenting spontaneous amelioration with aging. Hum Mol Genet 2001;10(21):2453-61.

Groves RW, Liu L, Dopping-Hepenstal PJ, Markus HS, Lovell PA, Ozoemena L, et al. A homozygous nonsense mutation within the dystonin gene coding for the coiled-coil domain of the epithelial isoform of BPAG1 underlies a new subtype of autosomal recessive epidermolysis bullosa simplex. J Invest Dermatol 2010;130(6):1551-7.

Ha C, Kim JW, Jang JH. Performance Evaluation of SpliceAI for the Prediction of Splicing of NF1 Variants. Genes (Basel) 2021;12(9).

Has C, Bauer JW, Bodemer C, Bolling MC, Bruckner-Tuderman L, Diem A, et al. Consensus reclassification of inherited epidermolysis bullosa and other disorders with skin fragility. Br J Dermatol 2020;183(4):614-27.

Has C, Bruckner-Tuderman L. The genetics of skin fragility. Annu Rev Genomics Hum Genet 2014;15:245-68.

Heagerty AH, Kennedy AR, Eady RA, Hsi BL, Verrando P, Yeh CJ, et al. GB3 monoclonal antibody for diagnosis of junctional epidermolysis bullosa. Lancet 1986;1(8485):860.

Hou PC, Natsuga K, Tu WT, Huang HY, Chen B, Chen LY, et al. Complexity of Transcriptional and Translational Interference of Laminin-332 Subunits in Junctional Epidermolysis Bullosa with LAMB3 Mutations. Acta Derm Venereol 2021;101(8):adv00522.

Jaganathan K, Kyriazopoulou Panagiotopoulou S, McRae JF, Darbandi SF, Knowles D, Li YI, et al. Predicting Splicing from Primary Sequence with Deep Learning. Cell 2019;176(3):535-48.e24.

Khan FF, Khan N, Rehman S, Ejaz A, Ali U, Erfan M, et al. Identification and Computational Analysis of Novel Pathogenic Variants in Pakistani Families with Diverse Epidermolysis Bullosa Phenotypes. Biomolecules 2021;11(5).

Kiritsi D, Kern JS, Schumann H, Kohlhase J, Has C, Bruckner-Tuderman L. Molecular mechanisms of phenotypic variability in junctional epidermolysis bullosa. J Med Genet 2011;48(7):450-7.

Matsui C, Nelson CF, Hernandez GT, Herron GS, Bauer EA, Hoeffler WK. Gamma 2 chain of laminin-5 is recognized by monoclonal antibody GB3. J Invest Dermatol 1995;105(5):648-52.

McGrath JA, Ashton GH, Mellerio JE, Salas-Alanis JC, Swensson O, McMillan JR, et al. Moderation of phenotypic severity in dystrophic and junctional forms of epidermolysis bullosa through in-frame skipping of exons containing non-sense or frameshift mutations. J Invest Dermatol 1999;113(3):314-21.

Moss C, Wong A, Davies P. The Birmingham Epidermolysis Bullosa Severity score: development and validation. Br J Dermatol 2009;160(5):1057-65.

Nakano A, Chao SC, Pulkkinen L, Murrell D, Bruckner-Tuderman L, Pfendner E, et al. Laminin 5 mutations in junctional epidermolysis bullosa: molecular basis of Herlitz vs. non-Herlitz phenotypes. Hum Genet 2002;110(1):41-51.

Nakano A, Pfendner E, Hashimoto I, Uitto J. Herlitz junctional epidermolysis bullosa: novel and recurrent mutations in the LAMB3 gene and the population carrier frequency. J Invest Dermatol 2000;115(3):493-8.

Pacho F, Zambruno G, Calabresi V, Kiritsi D, Schneider H. Efficiency of translation termination in humans is highly dependent upon nucleotides in the neighbourhood of a (premature) termination codon. J Med Genet 2011;48(9):640-4.

Posteraro P, De Luca N, Meneguzzi G, El Hachem M, Angelo C, Gobello T, et al. Laminin-5 mutational analysis in an Italian cohort of patients with junctional epidermolysis bullosa. J Invest Dermatol 2004;123(4):639-48.

Regev A, Teichmann SA, Lander ES, Amit I, Benoist C, Birney E, et al. The Human Cell Atlas. Elife 2017;6.

Rowlands C, Thomas HB, Lord J, Wai HA, Arno G, Beaman G, et al. Comparison of in silico strategies to prioritize rare genomic variants impacting RNA splicing for the diagnosis of genomic disorders. Sci Rep 2021;11(1):20607.

Stenson PD, Mort M, Ball EV, Chapman M, Evans K, Azevedo L, et al. The Human Gene Mutation Database (HGMD((R))): optimizing its use in a clinical diagnostic or research setting. Hum Genet 2020;139(10):1197-207.

Takeichi T, Nanda A, Liu L, Aristodemou S, McMillan JR, Sugiura K, et al. Founder mutation in dystonin-e underlying autosomal recessive epidermolysis bullosa simplex in Kuwait. Br J Dermatol 2015;172(2):527-31.

van den Akker PC, Jonkman MF, Rengaw T et al. The international dystrophic epidermolysis bullosa patient registry: an online database of dystrophic epidermolysis bullosa patients and their COL7A1 mutations. Hum Mutat 2011; 32: 1100-7.

Varki R, Sadowski S, Pfendner E, Uitto J. Epidermolysis bullosa. I. Molecular genetics of the junctional and hemidesmosomal variants. J Med Genet 2006;43(8):641-52.

Wang Z, Gerstein M, Snyder M. RNA-Seq: a revolutionary tool for transcriptomics. Nat Rev Genet 2009;10(1):57-63.

Journal Pre-proof

Case	Gender	Age	Zygosity	Gene				type
1	F	9 mo*	Homozygous	*LAMA3*	c.2038_2039dupAA	p.K680KfsX45	fs PTC	Severe
2	F	6 mo*	Homozygous	*LAMA3*	c.4338delG	p.L1446LfsX32	fs PTC	Severe
3	M	6 yr*	Homozygous	*LAMA3*	c.151insG	p.V51GfsX4	fs PTC	LOC
4	F	4 mo*	Heterozygous	*LAMB3*	c.727C>T, c.1903C>T	p.Q243X, p.R635X	Nonsense	Severe
5	F	21 yr	Homozygous	*LAMB3*	c.1702C>T	p.Q568X	Nonsense	Intermediate
6	M	7 yr	Homozygous	*LAMB3*	c.1186_1196del	p.T396CfsX12	fs PTC	Intermediate
7	F	19 mo*	Homozygous	*LAMB3*	c.2701+1G>A	N/A	Donor splice site mutation	Severe
8	F	2 mo*	Heterozygous	*LAMB3*	c.565-2A>G, c.2914C>T	N/A, p.R972X	Acceptor splice site and nonsense mutation	Severe
9	F	40 yr	Heterozygous	*LAMB3*	c.1705C>T, c.943+2T>C	p.R569X, N/A	Donor splice site and nonsense mutation	Intermediate
10	M	39 yr	Heterozygous	*LAMB3*	c.3119G>A, c.629-12T>A	p.W1040X, N/A	Acceptor splice site and nonsense mutation	Intermediate
11	M	23 yr	Homozygous	*LAMB3*	c.298+5G>C	N/A	Donor splice site mutation	Intermediate
12	F	11 mo*	Homozygous	*LAMC2*	c.132_135delCAGA	p.H44HfsX63	fs PTC	Severe
13	F	20 mo*	Homozygous	*LAMC2*	c.132_135delCAGA	p.H44HfsX63	fs PTC	Severe
14	M	6 yr	Homozygous	*COL17A1*	c.2910insT	p.P970SfsX8	fs PTC	Intermediate
15	M	16 yr	Homozygous	*COL17A1*	c.2910insT	p.P970SfsX8	fs PTC	Intermediate
16	M	6 yr	Homozygous	*COL17A1*	Large deletion of exons 16 and 17	Deletion of 81 amino acids	In frame large deletion	Intermediate
17	F	35 yr	Homozygous	*COL17A1*	Large deletion of exons 16 and 17	Deletion of 81 amino acids	In frame large deletion	Intermediate

Table 1: Genotypes of JEB cohort. Two individuals (12 and 13) had the same four nucleotide deletion in *LAMC2*, two individuals (14 and 15) had the same single nucleotide insertion in *COL17A1*, and two individuals (16 and 17) had the same large deletion in *COL17A1*. All individuals with severe JEB and LOC syndrome are deceased (marked with *). All individuals with intermediate JEB are alive at time of submission (May 2023).

Table 2 legend:

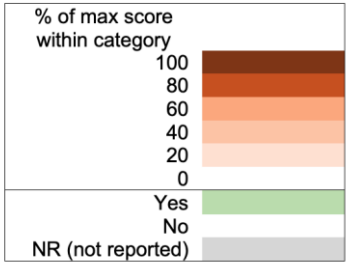

Case	BSA	Chronic wounds	Eyes	Larynx	Nails	Scarring alopecia	Teeth	Granulation tissue	Life threatening illness	Underweight (BMI <18.5)	Hypoalbuminaemia (35-50 g/L ref)	Anaemia (Hb <130 (males) or <120 (females) g/dL)	Mouth ulcers	Other comments
	Max score: 10	Max score: 5							Max score: 10					
5	4	2	2	0	5	4	4	4	0	Yes	Yes	Yes	Yes	Atrophic scarring
6	4	2	3	1	5	2	4	4	0	Yes	No	Yes	No	Atrophic scarring
9	0	0	1	0	2.5	0	4	0	0	No	NR	NR	Yes	10% non-scarring alopecia
10	3	2	2	0	5	3	3	0	0	No	Yes	No	Yes	Atrophic scarring
11	6	2	0	0	2.875	1	4	0	0	Yes	Yes	Yes	No	Atrophic scarring
14	2	0	1	0	3.5	0	0	0	0	Yes	No	Yes	Yes	
15	4	1	1	0	3.5	0	3	0	0	No	No	Yes	Yes	
16	5	2	1	2	4.375	2	0	0	1	Yes	Yes	Yes	Yes	Atrophic scarring
17	2	1	1	1	5	5	4	0	0	Yes	No	Yes	No	Atrophic scarring

Table 2: Phenotypes of intermediate JEB individuals**.** Scores of intermediate JEB cases from deep phenotyping. BSA = body surface area affected, this includes blisters, erosions, scabs, healing skin, erythema and atrophic scarring. This is given as a score out of 10. Life threatening illness was scored out of 10. All other categories are scored out of a maximum of 5 (see Figure 3). Further characteristics of intermediate JEB cases from deep phenotyping. NR = not reported.

Case	Zygosity	Mutation (*LAMB3*)	Exon skipping prediction	Cryptic splice site activation prediction	Predicted outcome comments	JEB subtype
7	Homozygous	c.2701+1G>A	Out-of-frame exon 18 skipping	19nt excluded from exon 18	Both outcomes out-of-frame	Severe
8	Heterozygous	c.565-2A>G, c.2914C>T (p.R972X)	Out-of-frame exon 7 skipping	117nt included from intron 6 (including TGA PTC at c.565-60)	1. In-frame cryptic activation with novel PTC introduced 2. Out-of-frame exon skipping	Severe
9	Heterozygous	c.1705C>T (p.R569X), c.943+2T>C	Out-of-frame exon 9 skipping	27nt included from intron 9	1. In-frame cryptic activation 2. Out-of-frame exon skipping	Intermediate
10	Heterozygous	c.3119G>A (p.W1040X), c.629-12T>A	Predicted to be unlikely	10nt included from intron 7	Out-of-frame cryptic splice site activation	Intermediate
11	Homozygous	c.298+5G>C	Out-of-frame exon 4 skipping	64nt included from intron 4	Both outcomes out-of-frame	Intermediate

Table 3: SpliceAI predicted resultant transcripts from splice site mutations. RT-PCR was performed for Case 11.

Journal Pre-proof

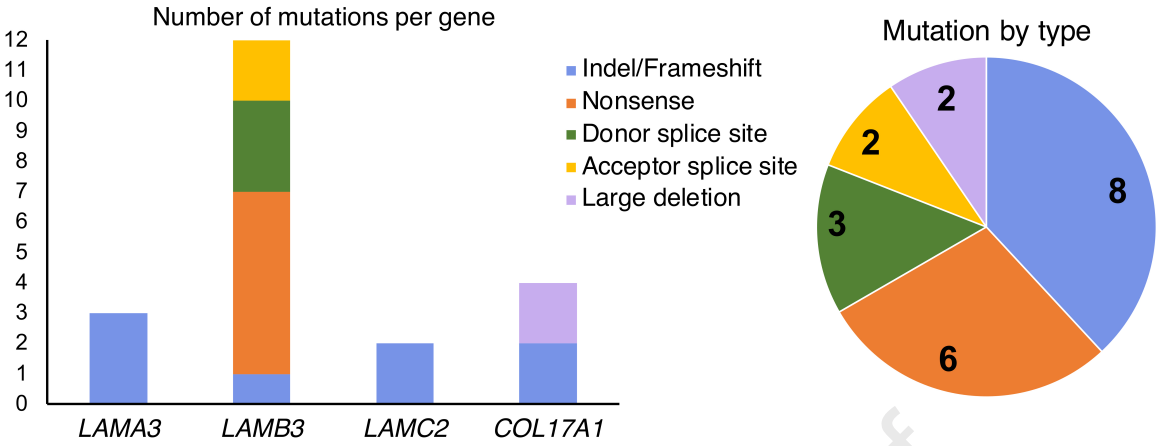

Journal Pre-proof

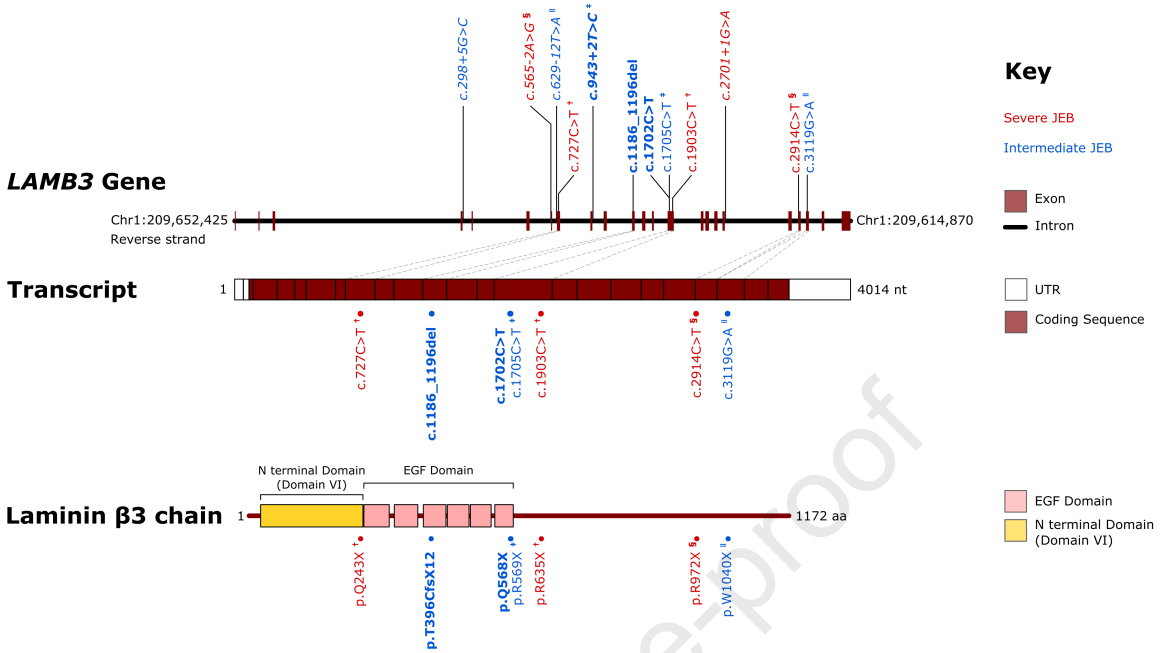

Journal Pre-proof

Journal Pre-proof

Journal Pre-proof

Area of body surface area (BSA) affected (%):

0	0%	6	51-60%
1	1-10%	7	61-70%
2	11-20%	8	71-80%
3	21-30%	9	81-90%
4	31-40%	10	91-100%
5	41-50%		

Chronic wounds (wounds present for >6 mo) (0-5)

0 None
1 1-10%
2 11-20%
3 21-29%
4 31-40%
5 41% or higher

Eyes (0-5)

Presence, extent and severity of:

- ☐ Conjunctival erythema and suffusion
- ☐ Corneal scarring (with end result = blindness in one or both eyes)
- ☐ Trichiasis and mechanical keratitis secondary to entropion formation
- ☐ Dryness secondary to ectropion formation
- ☐ Damage to the tear ducts

Larynx (0-5)

0 No problems from EB
1 Occasional hoarseness
2 Frequent hoarseness
3 Persistent hoarseness
4 Stridor
5 Laryngeal obstruction

Nails (0-5)

For score: Total lost nails ÷ 4 + total dystrophic nails ÷ 8

	Left hand	Right hand	Left foot	Right foot
Lost nails				
Dysmorphic				
Normal				

Scarring alopecia due to EB (0-5)

0 No alopecia
1 1-19% scalp involvement
2 20-39% scalp involvement
3 40-59% scalp involvement
4 60-79% scalp involvement
5 80-100% scalp involvement

Nutritional compromise (0-3)

- Height:_____
- Body weight:_____
- BMI:_____

☐ Underweight
☐ Hypoalbuminaemia
☐ Anaemia

Mouth (0-1)

☐ Soft tissue blisters and erosions

Teeth (0-5)

0 No problems from EB (normal teeth)
1 Localised or Generalised pitting
2 Enamel completely absent
3 Severe tooth wear and/or caries damage
4 Some teeth lost
5 All teeth lost

Granulation tissue (0-5)

0 None
1 <1% Body surface area
2 1-2% BSA
3 2-5% BSA
4 5-10% BSA
5 >10% BSA

Life threatening illness (0-10):

- ☐ Sepsis
- ☐ Renal failure
- ☐ Heart failure
- ☐ SCC

Total number of SCCs (up to 5):

SCC spread:

- ☐ No extracutaneous spread (0)
- ☐ Local/regional/LN spread (1)
- ☐ Distant metastatic spread (2)

- Other (freetext):

Other items for consideration (0-6):

- ☐ GU tract abnormalities
- ☐ Milia
- ☐ Hypertrophic or atrophic scarring
- ☐ Keratoderma
- ☐ Hyperhidrosis
- ☐ Absent dermatoglyphs (LOC)

Supplementary notes:

BSA affected includes:
Blisters, erosions, scabs, healing skin, erythema, atrophic scarring
Does not include:
Post-inflammatory pigmentation

Journal Pre-proof

Journal Pre-proof

Journal Pre-proof

Journal Pre-proof

Mutation	Gene	Strand	cDNA mutation	Exon or intron	GRCh37			GRCh38			Variant ID
					Location start	Location end	Accession number	Location start	Location end	Accession number	
1	*LAMA3*	+	c.2038_2039dupAA	Exon 17	Chr18:21487749	Chr18:21487750	NM_000227	Chr18:23907785	Chr18:23907786	NM_000227.6	New
2	*LAMA3*	+	c.4338delG	Exon 32	Chr18:21523890	Chr18:21523890	NM_000227	Chr18:23943926	Chr18:23943926	NM_000227.6	New
3	*LAMA3*	+	c.151insG	Exon 1	Chr18:21453159	Chr18:21453159	NM_000227	Chr18:23873195	Chr18:23873195	NM_000227.6	rs80356678
4a	*LAMB3*	-	c.727C>T	Exon 8	Chr1:209806023	Chr1:209806023	NM_000228	Chr1:209632678	Chr1:209632678	NM_000228.3	rs80356681
4b	*LAMB3*	-	c.1903C>T	Exon 14	Chr1:209799066	Chr1:209799066	NM_000228	Chr1:209625721	Chr1:209625721	NM_000228.3	rs80356682
5	*LAMB3*	-	c.1702C>T	Exon 14	Chr1:209799267	Chr1:209799267	NM_000228	Chr1:209625922	Chr1:209625922	NM_000228.3	New
6	*LAMB3*	-	c.1186_1196delACCGGGCAGTG	Exon 11	Chr1:209801482	Chr1:209801472	NM_000228	Chr1:209628137	Chr1:209628127	NM_000228.3	New
7	*LAMB3*	-	c.2701+1G>A	Intron 18	Chr1:209795880	Chr1:209795880	NM_000228	Chr1:209622535	Chr1:209622535	NM_000228.3	rs1553276110
8a	*LAMB3*	-	c.2914C>T	Exon 20	Chr1:209791389	Chr1:209791389	NM_000228	Chr1:209618044	Chr1:209618044	NM_000228.3	rs747916314
8b	*LAMB3*	-	c.565-2A>G	Intron 6	Chr1:209806480	Chr1:209806480	NM_000228	Chr1:209633135	Chr1:209633135	NM_000228.3	rs370148688
9a	*LAMB3*	-	c.1705C>T	Exon 14	Chr1:209799264	Chr1:209799264	NM_000228	Chr1:209625919	Chr1:209625919	NM_000228.3	rs201551805
9b	*LAMB3*	-	c.943+2T>C	Intron 9	Chr1:209803958	Chr1:209803958	NM_000228	Chr1:209630613	Chr1:209630613	NM_000228.3	New
10a	*LAMB3*	-	c.3119G>A	Exon 21	Chr1:209790864	Chr1:209790864	NM_000228	Chr1:209617519	Chr1:209617519	NM_000228.3	rs1057516759
10b	*LAMB3*	-	c.629-12T>A	Intron 7	Chr1:209806133	Chr1:209806133	NM_000228	Chr1:209632788	Chr1:209632788	NM_000228.3	rs754222671
11	*LAMB3*	-	c.298+5G>C	Intron 4	Chr1:209811874	Chr1:209811874	NM_000228	Chr1:209638529	Chr1:209638529	NM_000228.3	rs754529975
12	*LAMC2*	+	c.132_135delCAGA	Exon 2	Chr1:183177068	Chr1:183177071	NM_005562	Chr1:183207930	Chr1:183207933	NM_005562.3	rs1057516806
13	*LAMC2*	+	c.132_135delCAGA	Exon 2	Chr1:183177068	Chr1:183177071	NM_005562	Chr1:183207930	Chr1:183207933	NM_005562.3	rs1057516806
14	*COL17A1*	-	c.2910insT	Exon 44	Chr10:105798866	Chr10:105798866	NM_000494	Chr10:104039108	Chr10:104039108	NM_000494.4	New
15	*COL17A1*	-	c.2910insT	Exon 44	Chr10:105798866	Chr10:105798866	NM_000494	Chr10:104039108	Chr10:104039108	NM_000494.4	New
16	*COL17A1*	-	3010nt deletion from intron 15 to intron 17	Exons 16, 17	Chr10:105819014	Chr10:105816005	NM_000494	Chr10:104059256	Chr10:104056247	NM_000494.4	New
17	*COL17A1*	-	3010nt deletion from intron 15 to intron 17	Exons 16, 17	Chr10:105819014	Chr10:105816005	NM_000494	Chr10:104059256	Chr10:104056247	NM_000494.4	New

Table S1: Annotation of mutations. Mutation number corresponds to case number. Heterozygous mutations are labelled as a and b.

Architecture name	InterPro reference	Pfam reference	Start site	End site	Significance
LAMB3					
Laminin_N-terminal(Domain VI)	IPR008211	PF00055	26	248	6.30E-52
Laminin_EGF_domain	IPR002049	PF00053	250	305	3.10E-06
Laminin_EGF_domain	IPR002049	PF00053	316	367	6.20E-07
Laminin_EGF_domain	IPR002049	PF00053	379	428	5.40E-12
Laminin_EGF_domain	IPR002049	PF00053	431	478	1.80E-10
Laminin EGF domain	IPR002049	PF00053	481	526	1.20E-05
Laminin_EGF_domain	IPR002049	PF00053	534	574	8.70E-07
LAMA3A					
Laminin EGF domain	IPR002049	PF00053	78	122	1.30E-07
Laminin EGF domain	IPR002049	PF00053	125	175	3.60E-07
Laminin Domain I	IPR009254	PF06008	238	496	3.00E-92
Laminin Domain II	IPR010307	PF06009	679	807	9.50E-39
Laminin G domain	IPR001791	PF00054	826	961	1.70E-05
Laminin G domain	IPR001791	PF02210	1018	1133	3.60E-14
Laminin G domain	IPR001791	PF02210	1188	1292	3.60E-07
Laminin G domain	IPR001791	PF02210	1408	1526	1.20E-20
Laminin G domain	IPR001791	PF02210	1577	1701	9.80E-22
LAMA3B					
Laminin N-terminal (Domain VI)	IPR008211	PF00055	48	297	5.60E-75
Laminin EGF domain	IPR002049	PF00053	356	412	1.20E-05
Laminin EGF domain	IPR002049	PF00053	426	465	1.00E-06
Laminin EGF domain	IPR002049	PF00053	491	531	2.30E-08
Laminin EGF domain	IPR002049	PF00053	536	581	2.00E-09
Laminin EGF domain	IPR002049	PF00053	631	681	3.20E-07
Laminin EGF domain	IPR002049	PF00053	684	722	7.50E-05
Laminin EGF domain	IPR002049	PF00053	1266	1314	4.60E-10
Laminin EGF domain	IPR002049	PF00053	1356	1401	1.30E-09
Laminin EGF domain	IPR002049	PF00053	1405	1453	2.30E-08
Laminin B (Domain IV)	IPR000034	PF00052	1518	1652	1.40E-30
Laminin EGF domain	IPR002049	PF00053	1654	1677	0.014
Laminin EGF domain	IPR002049	PF00053	1687	1731	2.80E-07
Laminin EGF domain	IPR002049	PF00053	1734	1784	7.40E-07
Laminin Domain I	IPR009254	PF06008	1847	2105	7.20E-92
Laminin Domain II	IPR010307	PF06009	2288	2416	2.10E-38
Laminin G domain	IPR001791	PF00054	2435	2570	3.80E-05
Laminin G domain	IPR001791	PF02210	2627	2742	7.80E-14
Laminin G domain	IPR001791	PF02210	2797	2901	7.70E-07
Laminin G domain	IPR001791	PF02210	3017	3135	2.60E-20
Laminin G domain	IPR001791	PF02210	3186	3310	2.10E-21
LAMC2					
Laminin EGF domain	IPR002049	PF00053	28	81	8.00E-05
Laminin EGF domain	IPR002049	PF00053	84	128	7.00E-10
Laminin EGF domain	IPR002049	PF00053	139	184	2.80E-08
Laminin B (Domain IV)	IPR000034	PF00052	250	380	8.50E-28
Laminin EGF domain	IPR002049	PF00053	381	405	0.048
Laminin EGF domain	IPR002049	PF00053	462	504	2.70E-04
Laminin EGF domain	IPR002049	PF00053	517	570	1.20E-09
Laminin EGF domain	IPR002049	PF00053	573	604	0.0049
COL17A1					
Collagen triple helix repeat (20 copies)	IPR008160	PF01391	567	624	3.20E-08
Collagen triple helix repeat (20 copies)	IPR008160	PF01391	749	807	1.80E-09
Collagen triple helix repeat (20 copies)	IPR008160	PF01391	1438	1482	2.00E-07

Table S2: Predicted domains by InterPro. Significance scores greater than E-05 are highlighted in red and excluded from schematics

Journal Pre-proof

Case	Split location	Laminin-332 (GB3)	Laminin-332 (P3H9-2)	Collagen 4 (COL94)	Collagen 17 (NC16A-3)
1	Immunofluorescence mapping is consistent with a split through the lamina lucida.	Complete lack of laminin-332.	–	–	–
2	Cryostat sections show extensive blistering at or close to the dermal-epidermal junction (DEJ) Immunofluorescence mapping is consistent with a split through the lamina lucida.	Complete lack of laminin-332 immunoreactivity.	–	–	–
4	Immunofluorescence mapping indicates a split within the lamina lucida.	Complete absence of immunoreactivity to laminin-332 using the GB3 antibody.	–	–	–
5	Staining for collagen 4 with COL94 maps to the base of splits.	Very marked reduction in laminin-332 staining which is faint, interrupted and uneven compared to controls.	–	Staining is of similar pattern and intensity to the control.	–
7	No clear split or separation seen in sections viewed	Complete absence of labelling in contrast to bright linear staining in controls	–	Staining is of similar pattern and intensity to control skin	Staining is slightly reduced in comparison to controls with some minor discontinuities
8	No clear split or separation seen in sections viewed	Complete absence of immunostaining at the DEJ compared to bright linear staining in controls	–	Staining is of similar pattern and intensity to control skin	Staining is slightly reduced and patchy in comparison to controls
9	Occasional splits or detachment at or close to the dermal-epidermal junction (DEJ) on cryostat sections. Immunofluorescence mapping suggests a split close to the DEJ perhaps within the lamina lucida. Staining for laminin-332 with GB3 maps to the base of split areas. Staining for collagen 4 with COL94 maps to the base of splits.	Reduced and intermittent staining at the DEJ compared to controls.	–	Staining is of similar pattern and intensity to the control.	Reduced and intermittent labelling at the DEJ, similar to controls.
11	Most of the DEJ is intact with just a central microsplit evident. Staining for laminin-332 with GB3 and P3H9-2 maps to the base of split areas. Staining for collagen 4 with COL94 maps to the base of splits.	Patchy and substantially reduced staining in comparison to control.	Staining is reduced and of a similar pattern in comparison to control.	Staining is of similar pattern and intensity to the control.	–
13	–	Complete absence of laminin-332 immunoreactivity at the DEJ.	–	–	–
15	Immunofluorescence mapping shows a plane of cleavage in the lamina lucida of the basement membrane zone.	–	–	–	Absence of staining for type XVII collagen.

Table S3: Immunofluorescence mapping. DEJ = dermo-epidermal junction. Antibodies used are shown in brackets. Severe JEB cases are underlined. The Case 11 biopsy was from an area which was not noticed to blister

Journal Pre-proof

-D = 50nt		Delta scores				Positions			
Case	**Mutation**	**Acceptor Gain**	**Acceptor Loss**	**Donor Gain**	**Donor Loss**	**Acceptor Gain**	**Acceptor Loss**	**Donor Gain**	**Donor Loss**
7	c.2701+1G>A	0	0	0.37	0.99	20	22	20	1
8	c.565-2A>G	0.1	0.99	0	0	24	-2	-27	3
9	c.943+2T>C	0	0	0.32	0.99	-30	20	-25	2
10	c.629-12T>A	0.95	0.92	0	0	-2	-12	-13	-14
11	c.298+5G>C	0	0	0.01	0.93	-34	-1	-27	5
-D = 100nt		**Delta scores**				**Positions**			
Case	**Mutation**	**Acceptor Gain**	**Acceptor Loss**	**Donor Gain**	**Donor Loss**	**Acceptor Gain**	**Acceptor Loss**	**Donor Gain**	**Donor Loss**
7	c.2701+1G>A	0	0	0.37	0.99	20	22	20	1
8	c.565-2A>G	0.1	0.99	0	0.37	24	-2	67	-65
9	c.943+2T>C	0	0.05	0.32	0.99	-30	98	-25	2
10	c.629-12T>A	0.95	0.92	0	0	-2	-12	-13	83
11	c.298+5G>C	0	0	0.75	0.93	-34	98	-59	5
-D = 150nt		**Delta scores**				**Positions**			
Case	**Mutation**	**Acceptor Gain**	**Acceptor Loss**	**Donor Gain**	**Donor Loss**	**Acceptor Gain**	**Acceptor Loss**	**Donor Gain**	**Donor Loss**
7	c.2701+1G>A	0	0.26	0.37	0.99	20	145	20	1
8	c.565-2A>G	0.3	0.99	0	0.37	115	-2	67	-65
9	c.943+2T>C	0	0.41	0.32	0.99	-30	122	-25	2
10	c.629-12T>A	0.95	0.92	0	0	-2	-12	-13	83
11	c.298+5G>C	0	0.17	0.75	0.93	-34	119	-59	5
-D = 200nt		**Delta scores**				**Positions**			
Case	**Mutation**	**Acceptor Gain**	**Acceptor Loss**	**Donor Gain**	**Donor Loss**	**Acceptor Gain**	**Acceptor Loss**	**Donor Gain**	**Donor Loss**
7	c.2701+1G>A	0	0.26	0.37	0.99	20	145	20	1
8	c.565-2A>G	0.3	0.99	0	0.37	115	-2	67	-65
9	c.943+2T>C	0	0.41	0.32	0.99	-30	122	-25	2
10	c.629-12T>A	0.95	0.92	0	0	-2	-12	-13	83
11	c.298+5G>C	0	0.17	0.75	0.93	-34	119	-59	5
-D = 250nt		**Delta scores**				**Positions**			
Case	**Mutation**	**Acceptor Gain**	**Acceptor Loss**	**Donor Gain**	**Donor Loss**	**Acceptor Gain**	**Acceptor Loss**	**Donor Gain**	**Donor Loss**
7	c.2701+1G>A	0	0.26	0.37	0.99	20	145	20	1
8	c.565-2A>G	0.3	0.99	0	0.37	115	-2	67	-65
9	c.943+2T>C	0	0.41	0.32	0.99	-30	122	-25	2
10	c.629-12T>A	0.95	0.92	0	0	-2	-12	-205	83
11	c.298+5G>C	0	0.17	0.75	0.93	-34	119	-59	5
-D = 350nt		**Delta scores**				**Positions**			
Case	**Mutation**	**Acceptor Gain**	**Acceptor Loss**	**Donor Gain**	**Donor Loss**	**Acceptor Gain**	**Acceptor Loss**	**Donor Gain**	**Donor Loss**
7	c.2701+1G>A	0	0.26	0.37	0.99	20	145	20	1
8	c.565-2A>G	0.3	0.99	0	0.37	115	-2	67	-65
9	c.943+2T>C	0	0.41	0.32	0.99	-30	122	-25	2
10	c.629-12T>A	0.95	0.92	0	0	-2	-12	-205	83
11	c.298+5G>C	0	0.17	0.75	0.93	-34	119	-59	5
-D = 4999nt (max)		**Delta scores**				**Positions**			
Case	**Mutation**	**Acceptor Gain**	**Acceptor Loss**	**Donor Gain**	**Donor Loss**	**Acceptor Gain**	**Acceptor Loss**	**Donor Gain**	**Donor Loss**
7	c.2701+1G>A	0	0.26	0.37	0.99	627	145	20	1
8	c.565-2A>G	0.3	0.99	0	0.37	115	-2	67	-65
9	c.943+2T>C	0	0.41	0.32	0.99	2050	122	-25	2
10	c.629-12T>A	0.95	0.92	0	0	-2	-12	-205	1805
11	c.298+5G>C	0	0.17	0.75	0.93	-3891	119	-59	5

Table S4: SpliceAI predictions with varying settings for -D at 50, 100, 150, 200, 250, 350 and 4999 nucleotides. Changes in delta scores from one -D setting to the next are highlighted in red. Corresponding changes in positions of gain or loss sites are also highlighted.

Journal Pre-proof

Predicted splice site mutation outcomes

To evaluate whether the predicted splicing outcomes would result in PTCs, reference *LAMB3* transcript sequences were manually altered to the transcripts predicted by the tools by inserting or deleting DNA sequences that were predicted to be included or excluded by altered splicing. Sequences were translated into a primary amino acid sequence with ExPASY and aligned with the reference amino acid sequence using NCBI protein blast. All out-of-frame transcripts contained a PTC (Table S5), as did the in-frame insertion in Case 8. Here, cryptic splice site activation was predicted to result in the insertion of 117 additional nucleotides between exons 6 and 7, corresponding to 39 additional amino acids from position p.190 to p.228. However, a TGA stop codon is present at c.565-60, and results in a PTC at position p.208 (Figure 16). In contrast, the predicted in-frame transcript generated by cryptic splice site activation for Case 9 contained 9 amino acid insertion (RSFGSPLPW) without a PTC.

Transcript	Mutation	Consequence
7 exon skipping	c.2701+1G>A	p.I853TfsX32
7 cryptic splice site	c.2701+1G>A	p.V895PfsX4
8 exon skipping	c.565-2A>G	p.V189GfsX47
8 cryptic splice site	c.565-2A>G	p.V189ins19X
9 exon skipping	c.943+2T>C	p.V275GfsX81
9 cryptic splice site	c.943+2T>C	p.R315Sins9
10 exon skipping	c.629-12T>A	p.E210GfsX17
10 cryptic splice site	c.629-12T>A	p.E210GfsX51
11 exon skipping	c.298+5G>C	p.W62MfsX2
11 cryptic splice site	c.298+5G>C	p.D100GfsX56

Table S5: Translated splice site mutation predicted outcomes

Journal Pre-proof

-D = 58	Delta scores				Positions			
Position	**Acceptor Gain**	**Acceptor Loss**	**Donor Gain**	**Donor Loss**	**Acceptor Gain**	**Acceptor Loss**	**Donor Gain**	**Donor Loss**
209811874	0	0	0.01	0.93	-34	-1	-27	5

Table S6: Targeted analysis of surrounding region with -D of 58nt. Donor gain score and position is underlined.

Journal Pre-proof

Journal Pre-proof

	Delta scores				Positions			
Mutation	**Acceptor Gain**	**Acceptor Loss**	**Donor Gain**	**Donor Loss**	**Acceptor Gain**	**Acceptor Loss**	**Donor Gain**	**Donor Loss**
c.298+62A>T	0	0	0.94	0.15	71	-31	2	-2

Table S7: SpliceAI predictions for c.298+62A>T. Donor gain score and position is underlined.

Journal Pre-proof

Journal Pre-proof

		Delta scores				Positions			
Case	**Mutation**	**Acceptor Gain**	**Acceptor Loss**	**Donor Gain**	**Donor Loss**	**Acceptor Gain**	**Acceptor Loss**	**Donor Gain**	**Donor Loss**
5	c.1702C>T	0.1	0.04	0.01	0.01	-57	104	-1181	-183
6	c.1186_1196del	0.01	0.01	0	0.01	89	227	-320	493

Table S8: SpliceAI predictions for Cases 5 and 6 (-D = 4999nt)

Journal Pre-proof

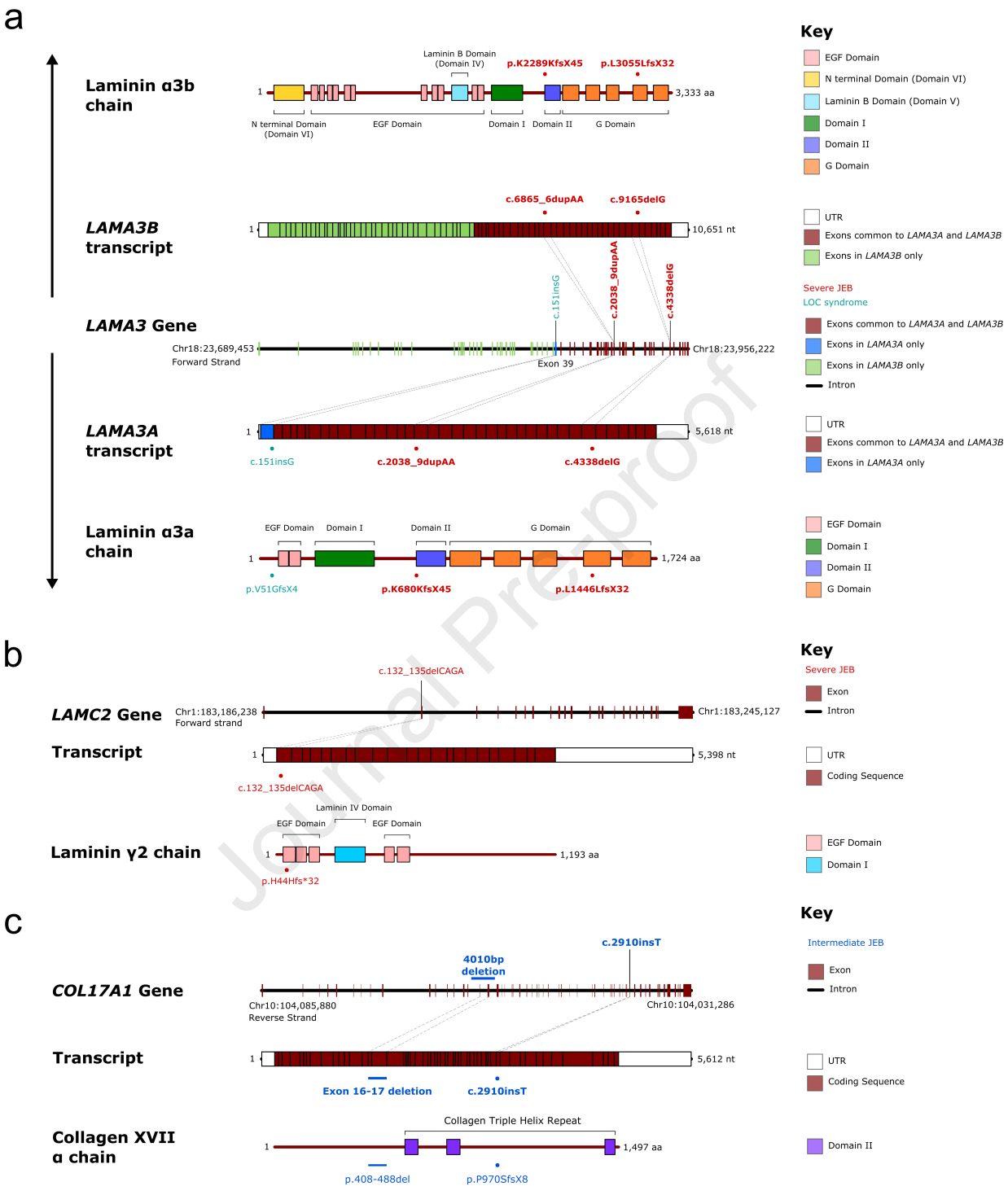

Journal Pre-proof

a

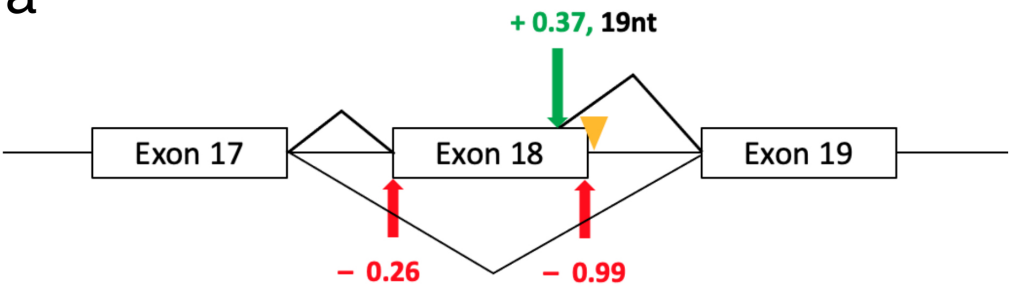

b

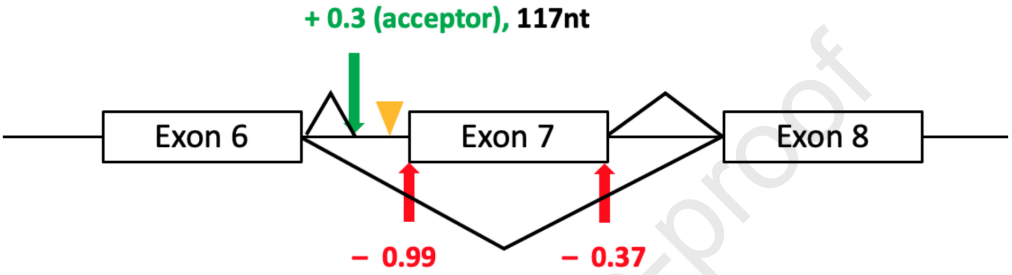

c

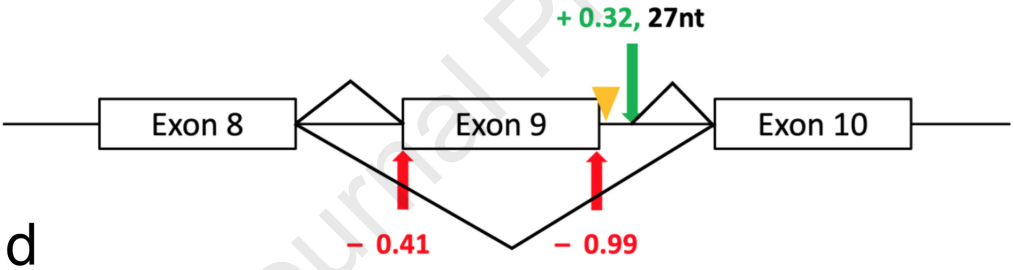

d

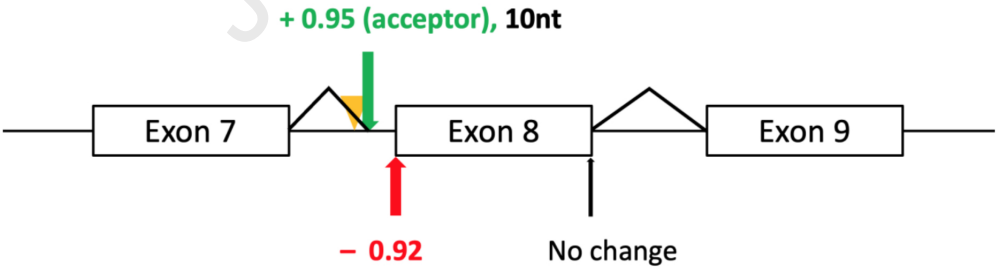

e

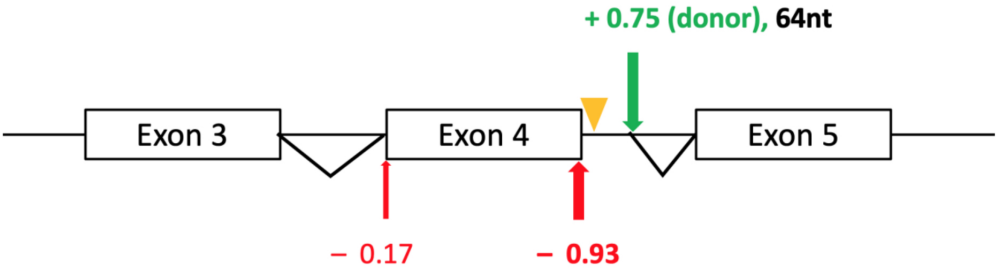

Journal Pre-proof

MRPFFLLCFALPGLLHAQQACSRGACYPPVGDLLVGRTRFLRASSTCGLTKPETYCTQYGEWQMKCC
KCDSRQPHNYYSHRVENVASSSGPMRWWQSQNDVNPVSLQLDLDRRFQLQEVMMEFQGPMPAGMLI
ERSSDFGKTWRVYQYLAADCTSTFPRVRQGRPQSWQDVRCQSLPQRPNARLNGGKVPGNKDFKCEA
YNGKKGFF-

Journal Pre-proof

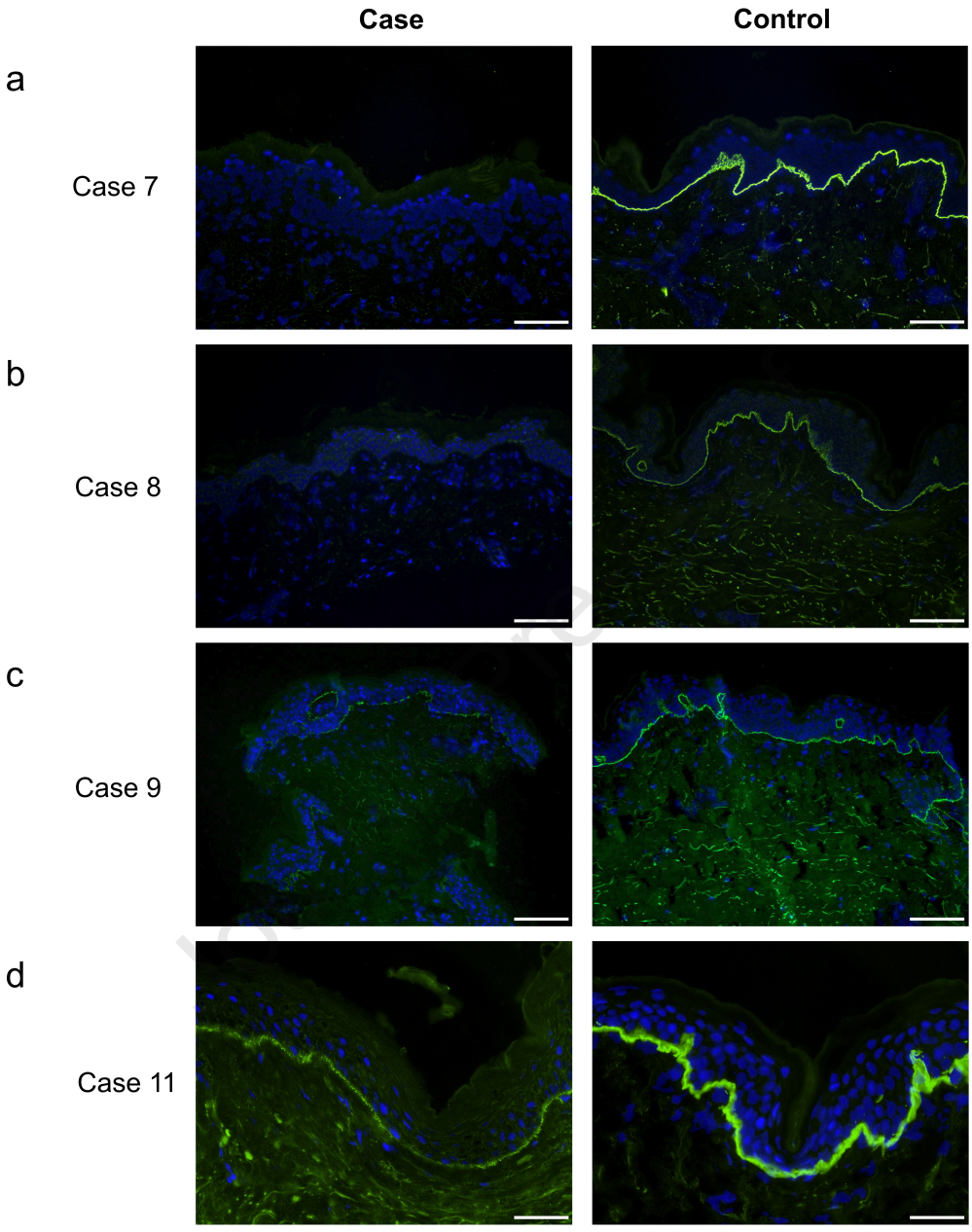
Case
Control
a
Case 7
b
Case 8
c
Case 9
d
Case 11

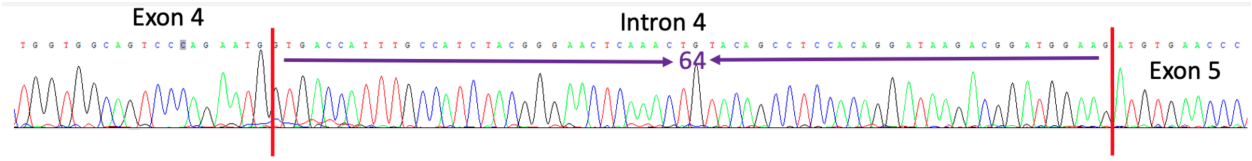

Journal Pre-proof

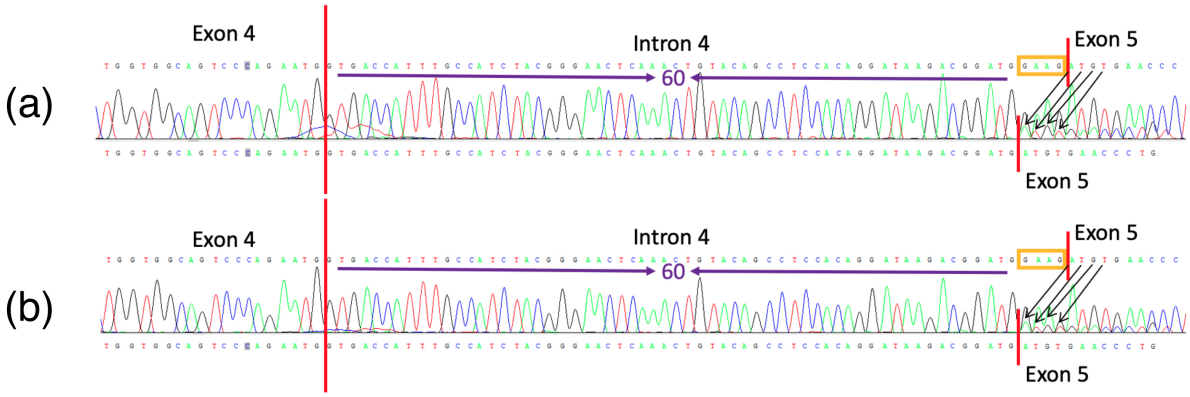

Journal Pre-proof

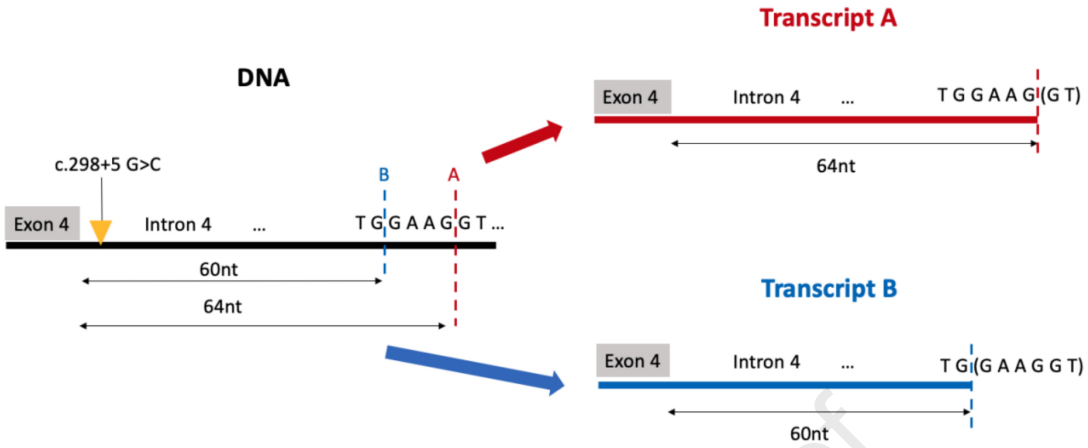

Journal Pre-proof

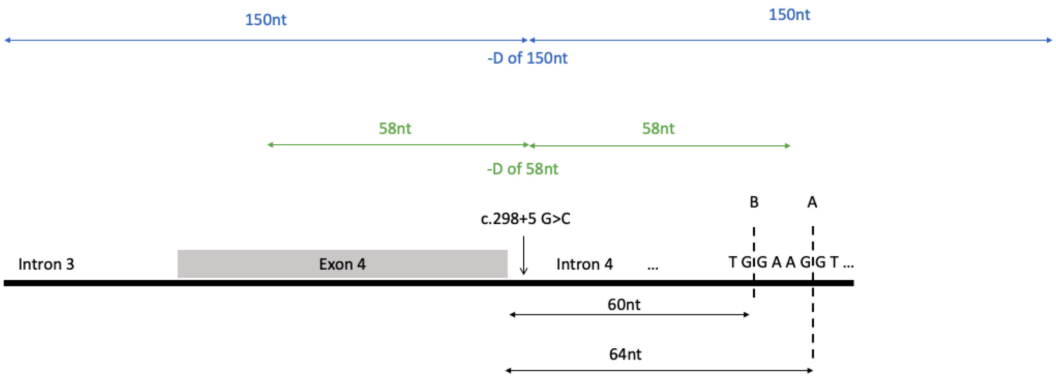

Journal Pre-proof

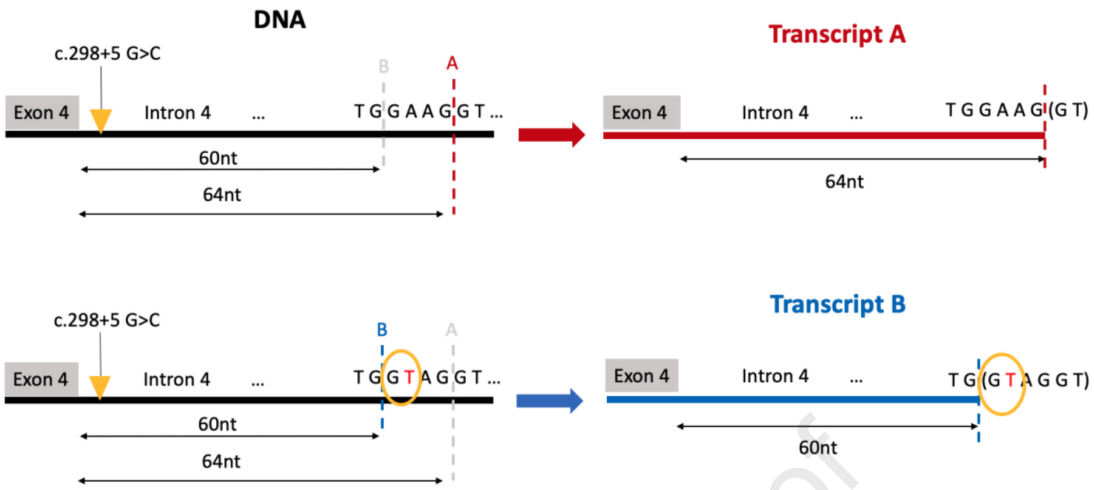

Journal Pre-proof

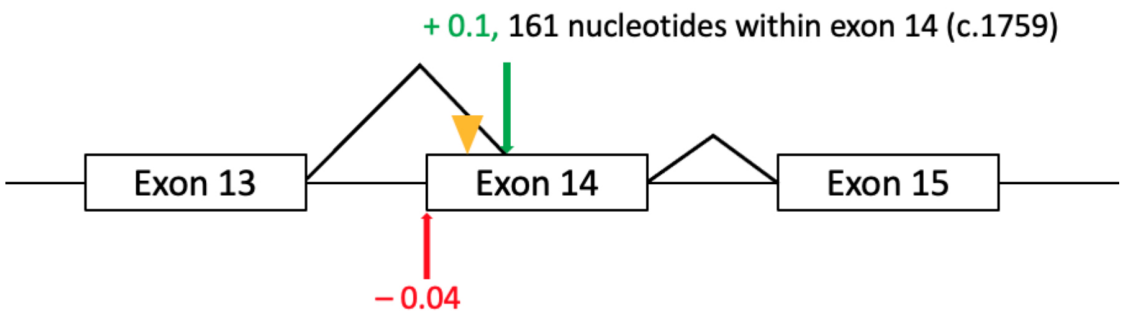

Journal Pre-proof

c.1186_1196del:

```
1168 GCTCCCTGTGACCCAGT GACCGGGCAGTGTG TGTGCAAGGAGCATGTGCAGGGAGAGCG CTGTGA
 390 -A--P--C--D--P--V -           -C --V--Q--G--A--C--A--G--R--A- -L--X-
```

c.1188_1198del:

```
1168 GCTCCCTGTGACCCAGT GACGGGGCAGTGTG TGTGCAAGGAGCATGTGCAGGGAGAGCG CTGTGA
 390 -A--P--C--D--P--V --T            --V--Q--G--A--C--A--G--R--A- -L--X-
```

Journal Pre-proof

Journal Pre-proof

SUPPLEMENTARY MATERIAL

Comparison with mutations reported in the literature:

Severe JEB

LAMA3

The two cases with *LAMA3* mutations were homozygotes for frameshift indels (p.K680KfsX45 and p.L1446LfsX32), and demonstrated a complete lack of laminin-332 immunoreactivity on IFM, consistent with an expected severe JEB phenotype. Possible explanations for the lack of staining include either NMD of transcripts, or truncated α3a chains that were unable to form laminin-332 heterotrimers.

p.K680KfsX45 has not been reported previously. A homozygous nonsense mutation (p.R782X) affecting the same domain (Domain II, residues 679–807) resulted in severe JEB too (Castori et al., 2008). p.L1446LfsX32 is also a previously unreported mutation; another homozygous exon 17 frameshift mutation (c.4335dupA, p.L1446IfsX11) similarly resulted in a severe JEB phenotype (Ayoub et al., 2005).

LAMB3

The genotype of Case 4 (p.Q243X/p.R635X) has been reported previously and is also associated with a severe JEB phenotype (Pulkkinen et al., 1997). The p.R635X mutation is the most common mutation associated with JEB in the laminin-332 genes, accounting for 45% of all *LAMB3* severe JEB cases (Nakano et al., 2000).

p.Q243X is also a recurrent mutation, accounting for 5.3% of all *LAMB3* severe JEB cases (Nakano et al., 2000). Homozygous genotypes of p.Q243X and p.R635X result in severe JEB (Nakano et al., 2000). Therefore, it is unsurprising this combination of mutations results in

severe JEB. This is reflected in the IFM findings of Case 4, where there was almost absent staining for laminin-332 in comparison to control.

LAMC2

The one *LAMC2* mutation identified in our cohort (H44HfsX63) resulted in severe JEB in two cases. This mutation mapped to exon 1, resulting in complete absence of laminin-332 immunoreactivity at the DEJ on IFM, consistent with severe JEB. This mutation is reported in ClinVar but is not linked to any publications in the literature. A similar case with a homozygous p.R95X mutation also resulted in complete absence of staining for laminin-332 with GB3 and severe JEB (Aberdam et al., 1994).

Intermediate JEB

COL17A1

In line with classical genotype-phenotype correlation paradigms, Cases 14, 15, 16 and 17 had intermediate JEB phenotypes. All *COL17A1* mutations in our cohort were previously unreported. Although the intron 15-17 deletion (exons 16 and 17, p.408-488) was in-frame, there was widespread skin and extracutaneous involvement. The COL17 transmembrane domain (p.467-489) is almost completely deleted, which may explain the relatively severe intermediate JEB phenotype. Herisse et al report a severe intermediate JEB phenotype with generalised blistering, nail and dental dystrophy and severe mucosal involvement secondary to a deletion from intron 16 to intron 17 (834 nucleotides, c.1268-267 to c.1465+369) which resulted in negative staining for COL17 on IFM (Herisse et al., 2021).

Journal Pre-proof

Regarding the previously unreported p.P970SfsX8 mutation, a similar p.G954AfsX112 (c.2860delG) mutation resulted in negative COL17 IFM, alopecia, dystrophic nails, oral blistering and generalised skin blistering (Kiritsi et al., 2011).

LOC syndrome

As expected, the homozygous c.151insG genotype in Case 3 resulted in LOC syndrome, and this individual passed away at six years of age following an out of hospital cardiac arrest. Although a PTC is introduced 7 nucleotides downstream of the mutation in exon 1, the transcript has been demonstrated to escape NMD as an alternative ATG start codon is utilised six exons downstream (McLean et al., 2003). The net overall is an N-terminal truncation of the laminin α3a polypeptide which lacks 226 residues, and this gives rise to the characteristic LOC phenotype.

Supplementary methods

Data visualisation

Identified pathogenic variants were mapped to the reference genome (GRCh 38) manually using the Ensembl genome browser.(Hunt et al., 2018) Existing general databases of genetic variants (ClinVar and HGMD Professional 2021.1) were searched to determine whether the mutation had been reported previously.(Landrum et al., 2018, Stenson et al., 2020) Schematics of genes and transcripts were constructed using genomic coordinates of the Homo sapiens genome assembly GRCh38 (hg38) imported from the Ensembl database.(Howe et al., 2021) Mutations identified were mapped onto gene, transcript and protein schematics with Inkscape Version 1.0.2 (Inkscape Project, Brooklyn, New York, USA) and an open-source R script,(Turner, 2015) in order to visualise and compare their locations. For protein schematics, domains were predicted using Interpro with e-values cut off at $<1E^{-3}$.(Blum et al., 2021)

Journal Pre-proof

Supplementary Figure Captions

Figure S1: Mutations identified in JEB cohort.
(a) Mutations identified in *LAMA3* and corresponding phenotypes. All individuals were homozygotes. Previously unreported mutations are shown in bold.
(b) Mutations identified in *LAMC2* and corresponding phenotypes. All individuals were homozygotes.
(c) Mutations identified in *COL17A1* and corresponding phenotypes. All individuals are homozygotes. Previously unreported mutations are shown in bold.

Figure S2: Schematic diagrams of predicted splicing outcomes from *LAMB3* mutations. The mutation is marked by a yellow triangle. Donor and acceptor loss scores are shown in red with (–). The donor gain score is shown in green with (+).
(a) Predicted splicing outcomes from Case 7 (c.2701+1G>A). The predicted cryptic donor splice site is 19 nucleotides from the original donor splice site.
(b) Predicted splicing outcomes from Case 8 (c.565-2A>G). The predicted cryptic acceptor splice site is 117 nucleotides from the original acceptor splice site.
(c) Predicted splicing outcomes from Case 9 (c.943+2T>C). The predicted cryptic donor splice site is 27 nucleotides from the original donor splice site.
(d) Predicted splicing outcomes from Case 10 (c.629-12T>A). The predicted cryptic acceptor splice site is 10 nucleotides from the original acceptor splice site.
(e) Predicted splicing outcomes from Case 11 (c.298+5G>C). The predicted cryptic donor splice site is 64 nucleotides from the original donor splice site.

Figure S3: Translated sequence of c.565-2A>G cryptic splice site transcript. Inserted amino acids secondary to cryptic splice site activation are shown in blue.

Figure S4: Immunofluorescence using GB3 antibody for laminin-332 in cases with *LAMB3* splice site mutations
(a) Case 7, complete lack of immunoreactivity compared with control skin
(b) Case 8, complete lack of immunoreactivity compared with control skin
(**c)** Case 9, reduced and intermittent staining at the DEJ compared to controls
(d) Case 11, patchy and substantially reduced staining in comparison to control.
Scale bars = 100μm for Cases 7, 8 and 9. Scale bar = 40μm for Case 11.

Figure S5: Sanger sequencing electrophoretogram of Case 11 *LAMB3* cDNA from blood confirming 64 additional nucleotides retained from intron 4 between exons 4 and 5 following aberrant splicing.

Figure S6: Sanger sequencing electrophoretogram of Case 11 *LAMB3* cDNA from **(a)** non-blistered skin and **(b)** blistered skin. An additional minor transcript (Transcript B) containing 60 retained nucleotides from intron 4 is evident in both. The GAAG nucleotides from position c.298+61 to c.298+64 are outlined in the orange box.

Figure S7: Cryptic splice site activation within intron 4 produces transcripts A and B. In this schematic diagram, the mutation c.298+5 G>C is marked by the yellow triangle. This disrupts the original exon 4-intron 4 donor splice site and results in utilisation of cryptic donor splice sites. Splicing at cryptic splice site A results in production of transcript A, where 64 additional nucleotides are included between exons 4 and 5. Splicing at cryptic splice site B

results in production of transcript B, where 60 additional nucleotides are included between exons 4 and 5.

Figure S8: Genomic regions analysed by -D of 58nt (green) and -D of 150nt (blue). With -D set at 58nt, c.298+64 is not considered for any delta score predictions as it is outside the considered area. Splice site A at c.295+64 corresponds with Transcript A. Splice site B at c.295+60 corresponds with Transcript B. Distances are not to scale.

Figure S9: A hypothesised second mutation (c.298+62 A>T), highlighted in the yellow circle, may produce a strong donor cryptic splice site at location B in a subpopulation of cells, resulting in transcript B.

Figure S10: Schematic diagram of predicted splicing outcomes from c.1702C>T

Figure S11: Aligned nucleotides and amino acids of Case 6 and c.1188_1198del. Homologous nucleotides and amino acids are in black text. Nucleotides and amino acids differing between the two cases are shown in orange. Deleted nucleotides are struck through. Stop codons are shown in red.

Journal Pre-proof

Supplementary Material References

Aberdam D, Galliano MF, Vailly J, Pulkkinen L, Bonifas J, Christiano AM, et al. Herlitz's junctional epidermolysis bullosa is linked to mutations in the gene (LAMC2) for the gamma 2 subunit of nicein/kalinin (LAMININ-5). Nat Genet 1994;6(3):299-304.

Ayoub N, Tomb R, Charlesworth A, Meneguzzi G. [Junctional epidermolysis bullosa. Identification of a new mutation in two Lebanese families]. Ann Dermatol Venereol 2005;132(6-7 Pt 1):550-3.

Blum M, Chang HY, Chuguransky S, Grego T, Kandasaamy S, Mitchell A, et al. The InterPro protein families and domains database: 20 years on. Nucleic Acids Res 2021;49(D1):D344-D54.

Castori M, Floriddia G, De Luca N, Pascucci M, Ghirri P, Boccaletti V, et al. Herlitz junctional epidermolysis bullosa: laminin-5 mutational profile and carrier frequency in the Italian population. Br J Dermatol 2008;158(1):38-44.

Herisse AL, Charlesworth A, Bellon N, Leclerc-Mercier S, Bourrat E, Hadj-Rabia S, et al. Genotypic and phenotypic analysis of 34 cases of inherited junctional epidermolysis bullosa caused by COL17A1 mutations. Br J Dermatol 2021.

Howe KL, Achuthan P, Allen J, Allen J, Alvarez-Jarreta J, Amode MR, et al. Ensembl 2021. Nucleic Acids Res 2021;49(D1):D884-D91.

Hunt SE, McLaren W, Gil L, Thormann A, Schuilenburg H, Sheppard D, et al. Ensembl variation resources. Database (Oxford) 2018;2018.

Kiritsi D, Kern JS, Schumann H, Kohlhase J, Has C, Bruckner-Tuderman L. Molecular mechanisms of phenotypic variability in junctional epidermolysis bullosa. J Med Genet 2011;48(7):450-7.

Landrum MJ, Lee JM, Benson M, Brown GR, Chao C, Chitipiralla S, et al. ClinVar: improving access to variant interpretations and supporting evidence. Nucleic Acids Res 2018;46(D1):D1062-D7.

McLean WH, Irvine AD, Hamill KJ, Whittock NV, Coleman-Campbell CM, Mellerio JE, et al. An unusual N-terminal deletion of the laminin alpha3a isoform leads to the chronic granulation tissue disorder laryngo-onycho-cutaneous syndrome. Hum Mol Genet 2003;12(18):2395-409.

Nakano A, Pfendner E, Hashimoto I, Uitto J. Herlitz junctional epidermolysis bullosa: novel and recurrent mutations in the LAMB3 gene and the population carrier frequency. J Invest Dermatol 2000;115(3):493-8.

Pulkkinen L, Meneguzzi G, McGrath JA, Xu Y, Blanchet-Bardon C, Ortonne JP, et al. Predominance of the recurrent mutation R635X in the LAMB3 gene in European patients with Herlitz junctional epidermolysis bullosa has implications for mutation detection strategy. J Invest Dermatol 1997;109(2):232-7.

Stenson PD, Mort M, Ball EV, Chapman M, Evans K, Azevedo L, et al. The Human Gene Mutation Database (HGMD((R))): optimizing its use in a clinical diagnostic or research setting. Hum Genet 2020;139(10):1197-207.

Turner TN. Plot Protein: Visualization of Mutations. 3.0.0 ed. https://github.com/tycheleturner/plot-protein2015